CHARACTERIZATION AND IDENTIFICATION OF LARGE EXTRACELLULAR VESICLES RELEASED BY HIV-1 INFECTED MYELOID AND T-CELLS

by

Fatemeh Dehbandi

A Thesis
Submitted to the
Graduate Faculty
of
George Mason University
in Partial Fulfillment of
The Requirements for the Degree
of
Master of Science
Biology

Committee:

_____	Dr. Fatah Kashanchi, Thesis Chair
_____	Dr. Ancha Baranova, Committee Member
_____	Dr. Alessandra Luchini, Committee Member
_____	Dr. Iosif Vaisman, Director, School of Systems Biology
_____	Dr. Donna Fox, Associate Dean, Office of Student Affairs & Special Programs, College of Science
_____	Dr. Fernando R. Miralles-Wilhelm, Dean, College of Science
Date: _____	Fall Semester 2021 George Mason University Fairfax, VA.

Characterization and Identification of Large Extracellular Vesicles Released by HIV-1 Infected Myeloid and T-cells

A Thesis submitted in partial fulfillment of the requirements for the degree of Master of Science at George Mason University

by

Fatemeh Dehbandi
Bachelor of Science
Azad University of Babol, 2016

Director: Fatah Kashanchi, Professor,
Department of Biology

Fall Semester 2021
George Mason University
Fairfax, VA

DEDICATION

This thesis is dedicated to my parents which their love and admiration for my passion in science throughout my life has always encouraged me to keep learning.

ACKNOWLEDGEMENTS

I would like to thank everyone in the Kashanchi lab, including Dr. Kashanchi for encouraging me to explore this topic, helping and supporting me during this thesis and entirely my master program. Yuriy, for being a patience mentor and helping me in my experiments, Sarah for all of her kind support during my master program, and Gwen for always keeping me in loop.

TABLE OF CONTENTS

LIST OF FIGURES

Figure **Page**

LIST OF ABBREVIATIONS

Human Immunodeficiency Virus Type 1 ..... HIV-1
EVs..... Extracellular vesicles
PHA..... Phytohemagglutinin
IL-2……Interleukin-2
cART.....Combination antiretroviral therapy
TAR.....Transactivation response
ESCRT ..... Endosomal sorting complex required for transport
HAND..... HIV-1-associated neurocognitive disorder
RT-qPCR.....Real-time quantitative polymerase chain reaction
NTA .....Nanoparticle tracking analysis
Cell-free DNA.....cfDNA
Pathogen Associated Molecular Pattern .....PAMP
Damage Associated Molecular Patterns .....DAMP
Polymerase Chain Reaction .....PCR
kilodalton .....kDa
Figure ..... Fig.
Combined antiretroviral therapy .....cART
LEs .....Late endosomes
MVBs.....Multivesicular bodies
LAMP1……Lysosomal-associated membrane protein
LC3 ..... Microtuble-associated proteins 1A/1B light chain
3 SNAREs.....Soluble N-ethylmaleimide-sensitive factor activating protein receptors
Rab .....Ras-related protein
EEA1..... Early Endosome Antigen 1

ABSTRACT

CHARACTERIZATION AND IDENTIFICATION OF LARGE EXTRACELLULAR VESICLES RELEASED BY HIV-1 INFECTED MYELOID AND T-CELLS

Fatemeh Dehbandi, M.S.

George Mason University, 2021

Thesis Director: Dr. Fatah Kashanchi

The mounting evidences suggest that extracellular vesicles (EVs) contribute to HIV-1 pathogenesis, which is likely attributed to their ability to carry viral proteins and RNA. Previously we were able to investigate the role of EVs in viral infections [1] [2] [3] [4] [5]. Since EVs are heterogenous in their sizes and intracellular origin [6], we have attempted to investigate the role of large EVs in HIV-1 infection. HIV-1 infected monocytes and T cells were synchronized in G0 phase by serum starvation for 72 hours. Afterwards, cells were released in serum-rich media containing inducers to initiate viral transcription and resume normal cell cycle. The supernatant samples were collected at prior to release (-72 hours), and then, 6 (+6 hours) and 24 (+24 hours) post release. To enrich the samples for large EVs, the supernatants were centrifuged at 2000g (2K) speed for 45 minutes and separated through size exclusion chromatography and tested for viral proteins and RNAs. As a result, 2K fractions from both infected myeloid and T-cells showed the presence of HIV-1 capsid and envelope proteins, as well as HIV-1 short non-

coding RNA (TAR). Next, the isolated large EVs from both infected myeloid and T-cells were subjected to virus rescue assay on uninfected naïve myeloid and T-cells. The cells were lysed and tested on the presence of viral proteins. As a result, previously uninfected myeloid and T-cells showed the production of viral proteins after the treatment by 2K EVs collected from -72 hours samples and +24 hrs. The cell treated by +6 hours, on the other hand, did not produce viral proteins. Taken together, 2K fraction from HIV-1 infected myeloid and T-cells, collected at 24 hours post release and from serum-deprived cells, are infectious and contain fully fledged virions. However, large EVs collected at 6 hours post-release failed to initiate viral infection. Since, 2K samples, including non-infectious ones, contain short non-coding HIV-1 RNA (TAR), they might play a major role in bystander effect on uninfected neighboring cells, that was reported previously [1].

INTRODUCTION

Human immunodeficiency virus type 1 (HIV-1), the primary agent of acquired immunodeficiency syndrome (AIDS), has remained a major public health concern worldwide since its discovery at the beginning of 1980s [7]. Approximately 37.6 million people are infected with HIV-1 globally which35.9 million were adults and 1.7 million were children (<15 years old). [8] . Although there are no permanent treatments for HIV/AIDS, the development of combination antiretroviral therapy (cART) has dramatically improved the quality of life of HIV-1 patients and reduced the incidence of HIV-1-related opportunistic infections. By the end of 2020, 24.7 million HIV-1 patients (73%) are receiving cART [8]. Drugs that target several stages of the HIV-1 life cycle, such as viral fusion, reverse transcription, integration, viral polyprotein cleavage, and virion maturation, are included in antiretroviral therapy combinations [9]. Albeit cART does not totally eliminate the virus, it does suppress it by decreasing the viral load in plasma to undetectable levels and demands adherence to a stringent regimen for the rest of one's life. As a result, failure to adhere to medication or the withdrawal of cART allows the virus to reactivate [10]. cART causes infected cells to enter a state of latency which is one of the most significant obstacles to eradicating the virus in HIV-1 [11]. Through the fusion of the provirus into the genome, HIV-1 creates viral reservoirs and

survives in infected cells. Patients on cART have been reported to produce low quantities of viral RNA in CD4+ T cells and multiple brain areas, indicating that latent reservoirs, notably in resting memory CD4+ T cells and macrophages, are not fully silent [12] [13]. CD4+ T cells and macrophages both express the CD4 molecule and also the chemokine receptor CCR5 on their cell surfaces, which HIV-1 uses to enter cells. Viral binding and entry are the first steps in the viral life cycle [14] [15]. As the virus approaches the target cell, the viral protein gp120 binds to both CD4 and CCR5 in a sequential manner, causing fusion of the virus and plasma membranes. After fusing, the viral core travels through the cytoplasm, where it begins reverse transcribing its RNA genome into double-stranded DNA, which it then integrates into the host cell genome via the viral enzyme Integrase. Transcription leads to the early synthesis of regulatory HIV-1 proteins, which aid in the generation of longer RNA transcripts. After emerging from the host cell plasma membrane, these newly structured proteins are assembled at the cell surface and discharged as a new, mature virion [14] [15]. Both the infecting virus and the host's immunological response to the virus contribute to the pathogenesis of HIV-1 infection. Direct exposure is required for viral transmission, which is highly dependent on the virus isolation, concentration, and host sensitivity. The virus is disseminated into the regional lymph nodes and then into the bloodstream by CD4+ T cells, which are the first to be infected [14] [15]. Dendritic cells, CD4+ T cells, and macrophages all could be susceptible to get infected by virus particles. Infected cells usually succumb to the infection, either dying or developing a latent infection. The number of CD4+ T cells significantly decreases during this stage of infection as virus titers swiftly rise, although

this reaction is short-lived as the host generates humoral and cellular immune responses. HIV-1 RNA levels decrease and CD4+ T-cells increase as a result of Antibody-Dependent Cellular Cytotoxicity, which is mediated by Natural Killer T-cells, HIV-specific T-cells, and antibodies. HIV-1 pathogenic effects remain, resulting in the steady loss of CD4+ T cells and viral dissemination inside lymphoid settings. Patients develop AIDS in the absence of treatment and often succumb to opportunistic infections as a result of their weakened immune system [14] [15].

Extracellular vesicles (EVs), have been proven to contribute to viral persistence. EVs are a heterogenous group of membrane-bound vesicles that arise from either the endosome or the plasma membrane. The release of EV is a key mediator of intercellular communication that plays a role in both normal physiological and pathological processes. EVs have been categorized into three main group based on the size: Exosomes are described as small EVs with a diameter of 30-150 nm, microvesicles as medium EVs with a diameter of 100 nm-1 μm, and large EVs which include apoptotic bossies with a diameter 150 nm-5 μm [16]. Extracellular vesicles can be secreted directly from the plasma membrane and released via the endocytic pathway, or they might be the consequence of autophagic unconventional secretion. Exosomes are generated intracellularly within multivesicular bodies of the early endosome system [17], and microvesicles are produced by plasma membrane blebbing and "pinching-off" of plasma membrane and cytoplasmic material [18]. Studies investigating the characterization of small and medium-sized EV populations with certain cargo-type are also being conducted. The transmembrane tetraspanin protein family, which comprises CD9, CD63,

and CD81, is found in both exosomes and microvesicles [19]. Ongoing study show that, these proteins are involved in EV production and may provide further information about particular EV intracellular origin and selective cargo packaging [20]. Cargoes are usually regarded as being present on the membrane surface or within the EV lumen [21]. Many small EVs/exosomes have been found to carry particular proteins that cause physiological changes in recipient cells when they interact with exosomes [22]. Exosomes also include biologically active chemicals such as cytokines, chemokines, and interferons [23], Large number of RNA [24], as well as other molecules, can trigger an inflammatory response in recipient cells. Exosomes and microvesicles have also been found to transport mitochondrial DNA [25], single-stranded DNA [26], double-stranded DNA [27], chromatin [28], and other nuclear-derived components [29]. Secreted autophagosomes of the autophagy system, which carry distinct cargoes that have eluded lysosomal hydrolysis and persist in the extracellular environment, are another mechanism that might be included in this heterogeneous population of exosomes and microvesicles [30].

Concerning the Large EVs, Apoptotic bodies emerge during coordinated blebbing events, which correlate to the controlled cell death mechanisms seen in apoptosis [31], whereas oncosomes, the other large EVs category, are formed by cancerous cells blebbing off portions of the plasma membrane and usually carry cargoes capable of increasing the lethality of the original tumor site [32]. These larger EV subtypes are distinct to the processes from which they are produced and to the disease state from which they emerge, especially in the case of oncosomes originated from different cancer tumor environment, where they may be useful as future oncogenic biomarkers [33].

Large EVs Biogenesis

Large EVs play crucial role in a large numbers of cancers such as, breast cancer [34], prostate cancer [35], glioma [36], glioblastoma [37], colon cancer [38], pancreatic [39] cancer, melanoma [40] and leukemia [41]. In other words, all cancer cells produce large EVs, which their components differ from those produced by normal cells or the tumor microenvironment [42]. Nonetheless, only a few large EV populations, such as large oncosome, also known as LO, have been identified as specifically secreted by cancer cells [43]. Signaling pathways are triggered by both biochemical composition and biophysical mechanisms, which drive large EV biogenesis and shedding. The modulation of plasma membrane (PM) flexibility by cells, which is dependent on different lipid/protein combinations, is one of the most important aspects to consider in large EVs PM-derived biogenesis investigations [44]. Studies have shown that the mechanisms underlying the biogenesis of large EVs from Red Blood Cells, identifying four key factors: 1) the dynamics of the cytoskeleton 2) Viscosity of cytoplasm 3) The ions equilibrium 4) Biological process. All of these factors are involved in the longevity and proliferation of nucleated-cancer cells, and some of them have been attributed to the shedding of large EVs in recent studies [45]. Changes in cytoskeleton dynamics associated with the development of aggressive characteristics in Prostate Cancer (PCa) cells resistant to mevalonate pathway inhibitors and then led to an increase in large oncosome shedding [44].

Silencing of the gene encoding the cytoskeletal regulator Diaphanous related formin-3 (DIAPH3) has been demonstrated to enhance LO shedding, which in turn

boosts the amoeboid phenotype. Studies revealed that extracellular matrix degradation products can impact intracellular calcium influx and cytoskeleton remodeling, promoting a tumor amoeboid phenotype [46]. However, cell viscosity was first investigated in tumor cells versus normal cells, it has recently been linked to chemo-resistance and enhanced EV shedding. In terms of ions balance, Ca2+ levels regulate large EV shedding when flippases and other proteins involved in lipid bilayer asymmetry are activated. The development of membrane blebbing and the exposure of phosphatidylserine (PS) to the exterior leaflet are determined by the Ca2+-dependent activation of calpains [44]. Although tetraspanins are commonly suggested as exosome biomarkers, specific tetraspanins can also induce PM curvature and they have been identified in shedding vesicles. It is important to bear in mind that RAS super family GTPases are supposed to be essential mediators in the formation of the large EVs .Through the downstream signaling of ROCK (Rho-associated coiled-coil containing kinases) and ERK (extracellular signal-regulated kinases), activated RhoA enhances actin-myosin contraction, which is deemed necessary for large EV formation, and similar process have been discovered for LO biogenesis [44]. The formation of large EVs may potentially be modulated by endosomal sorting complexes necessary for transport (ESCRT). This pathway was presumed to be crucial only for exosome synthesis from the endosomal membrane at first. Nonetheless, some ESCRT proteins (such as TSG101 and VPS4 ATPase) have been shown to be able to move from the endosomal membrane to the PM, where they regulate the release of large EV. Furthermore, stimulation of the epidermal

growth factor receptor (EGFR) and overexpression of a membrane-targeted, have been associated to LO shedding [35].

Content of Large EVs

Protein

The GTPase ADP-ribosylation factor 6 (ARF6) has been found in LO which its activation stimulates the recruitment of ERK to the PM, allowing actomyosin contraction at the necks of large EVs and thereby their release. According to previous research on PM-derived large EVs, LO also contain caveolin-1 and metalloproteinases 2–9 (MMP2, 9). Furthermore, keratin 18 (CK18, a type I cytokeratin) seems to be abundant in large EVs, and has been utilized to demonstrate LO-like structure in human PCa tissues and bodily fluids [44]. Some specific enzymes associated with cancer cells metabolism including glyceraldehyde 3-phosphate dehydrogenase (GAPDH), glucose phosphate isomerase (GPI), heat shock 70 kDa protein 5 (HSPA5), malate dehydrogenase (MDH), aspartate transaminase (GOT), and lactate dehydrogenase B (LDHB), have been recently found to be significant in LO from PCa cell lines in comparison to the exosomes from the same source. Moreover, Glutaminase (GLS), a cytoplasmic enzyme that converts glutamine to glutamate, was shown to be one of the proteins expressed exclusively in large EVs [33]. So far, membrane proteins indicate 30% of all proteins discovered in both large and small populations of EVs. While tetraspanins and cell adhesion proteins were found to be abundant in small EVs, a bioactive alpha V (V)-integrin was discovered on the surface of LO from an aggressive model of PCa resistant to mevalonate pathway inhibitors. The transfer of adhesion and invasion functionality from the PCa aggressive

cell line to the less aggressive counterpart is mediated by this LO-associated V integrin. Additionally, a considerable amount of LO was found in the two proteins associated with cancer progression, urokinase-type plasminogen activator receptor (uPAR) and eukaryotic elongation factor 1 gamma (eEF1γ), which secreted by aggressive counterpart [44]. Despite of unclear characteristics of protein cargo in distinct population of EVs, it has been assumed that aggressive PCa cells may selectively load particular proteins in LO rather than small EVs in order to accelerate cancer progression by improving cell-to-cell communication. Furthermore, the presence of ongoing AKT1 kinase activity in prostate cancer, confirming this population's role as an effective signaling platform. Interestingly, active AKT1 was detected in circulating EV from the plasma of metastatic prostate cancer patients and was LO specific [44].

Nucleic acid

A diverse RNA cargo, including mRNAs, microRNAs, and noncoding RNAs (ncRNAs) were discovered in EVs content. Large EVs contain higher quantities of caveolin-2 (CAV2) and glutathione S-transferase pi 1 gene (GSTP1) transcripts than exosomes, indicating that mRNA cargo differs not only by EV cellular origin but also by subpopulation, with each subpopulation carrying a distinct level of the cell transcriptome [44]. Upon evaluating different EV subtypes secreted from a human colon cancer cell line, different microRNA-enrichment patterns were discovered. MicroRNA biogenesis, on the other hand, may be correlated to endosomal/exosome processing. Although single-stranded DNA (ssDNA) and mitochondrial DNA have only been studied frequently in exosomes, large EVs have been found to include retrotransposons and amplified

oncogene sequences [44]. Since, LOs carry miRNA, mRNA, and DNA, they also may similarly to other EVs promote horizontal movement of nucleic acids species inside and between tissue compartments, as well as to distant locales, via the circulation. Morello et al. in 2013, discovered that overexpression of miR-1227 in RWPE-2 PCa cells resulted in preferential loading of the miRNA into LO rather than smaller EVs, and overexpression of this protein in LO was found to be a new regulator of the migration of cancer-associated fibroblasts (CAFs). It has been recently discovered that large EVs produced from PCa patient plasma particularly contain circulating DNA. Furthermore, the presence of copy number variations of genes mostly altered in metastatic PCa (i.e. MYC, AKT1, PTK2, KLF10, and PTEN) in large EVs, as genetic aberrations related to the cell of origin, revealing that LO might be used as biomarkers in a liquid biopsy approach [32] [44]. Immune-flowcytometry of the purified vesicles from patients with prostate cancer has indicated that large oncosomes expressing Caveolin-1 can reveal metastatic disease. According to Morello et al. data, the amount of Cav-1 large oncosomes derived from plasma corresponds to disease progression. Same study discovered that large oncosomes detected in situ in prostate cancer tissues could be used to distinguish between aggressive and non-aggressive disease [32].

Taylor et al. investigated for miRs in tumor tissue and serum-derived tumor-specific exosomes in ovarian cancer patients. qRT-PCR was used to validate those miRs that were present in both the tumor and exosomes and had earlier been detected as overexpressed in human ovarian cancer, revealing a direct association between the tumor and tumor-derived exosomes [47]. In exosomes obtained from patients diagnosed with

early and late stage ovarian cancer, all of these miRs were significantly higher than in exosomes collected from patients diagnosed with benign ovarian disease; However, in late-stage malignancies, miR-200c and miR-214 were shown to be present in larger copy quantities. When plasma samples from breast cancer patients are compared to healthy women, the levels of circulating let-7a and miR-195 are dramatically higher [48]. In comparison to normal tissue, these miRs were likewise overexpressed in the tumor. Both of the previously stated miRs may also operate as biomarkers of therapeutic response, as their post-operative levels were equivalent to healthy women's blood samples. In prostate cancer patients, circulating miR-141 levels are higher than in healthy people. Moreover, circulating miR-141 and miR-375 (both of which are higher in prostate cancer specimens than in normal tissue) have been linked to metastatic cancer. A pro-invasive signature was discovered in analyses of miRs identified in large oncosomes in prostate cancer [48].

Lipid

Several fatty acids, including ceramide and phosphatidylserine, are abundant in large EVs, suggesting that they play a structural or functional role in vesicle production [49]. The phospholipid membrane of large EVs also contains active signaling lipids. ATP-stimulated microglia, for instance, can secrete large EVs carrying the endocannabinoid N-arachidonoyl-ethanolamine (anandamide), which stimulates the Cannabinoid Receptor-1 (CB1) and triggers metabolic alterations in recipient cells. Lipid expression on large EVs can be modulated by cells, based on the role they are dedicated to [49]. Recent studies indicate that large EVs derived from platelet, for instance, can utilize extracellular phospholipase A2 and vesicular 12-lipoxygenase to transform their

membrane lipids into the signal molecule 12-HETE (12-hydroxy eicosatetraenoic acid) at inflammatory areas. The 12-HETE appears to be involved in the internalization of large EVs by neutrophils, resulting in their activation in situ. Since a 12-HETE receptor, the BLT2, has been involved in cancer cell alteration, invasion, and metastasis, and also VEGF-mediated angiogenesis, cancer cells could utilize a similar process [49].

Role of Large EVs in Cancer

Cancer cells can vesiculate in a number of ways, including augmented EV emission, changes in size, shape, and molecular composition, and changes in biological activity. Some of these abnormalities could be the result of disease-related modifications in the EV biogenesis pathways, which D'Asti et al. term to as neovesiculation [48]. Several mechanisms have distinguished the EVs released by cancer cells from that of their non-transformed counterparts. In prostate cancer, for example, deregulation of the Akt pathway, growth factor stimulation (EGF), and lack of the diaphanous related formin 3 (DRF3), results in the emergence of a cellular phenotype related to invasiveness, amoeboid motility, and a distinct form of neovesiculation. The unique form of neovesiculation is characterized by the production of large membrane blebs on the cell surface, which are eventually splitted into large oncosomes [48]. The biological activities of large oncosomes are associated with their chemical content of signaling, and their formation could be considered as a marker of prostate cancer aggressiveness associated with a loss of a putative tumor suppressor (DRF3) [43]. Transforming miR species, oncogenic transcripts, active oncoproteins, and genomic regions encoding mutant oncogenes are just a few of the cancer-related substances that can be found in oncosomes.

Al-Nedawi et al. demonstrated that a shortened and carcinogenic form of the EGFR, EGFR variant III (EGFRvIII), may be transferred across Glioblastoma multiforme (GBM) cells via membrane-derived microvesicles, resulting in its accumulation on the cell surface [50] [49]. This causes an abnormal stimulation of the MAPK signaling pathway, resulting in dysregulation of EGFRvIII downstream genes such as VEGF and Bcl-xL anti-apoptotic up-regulation and p27 cyclin-dependent kinase inhibitor down-regulation. By decreasing apoptotic triggers in recipient cells, these modifications accelerate GBM cell morphological transformations and enhance anchorage-independent growth and pro-angiogenic activity. In addition, large EVs have the ability to transmit large DNA molecules to recipient cells, enhancing their tumorigenic potential. Vesicles produced by these cells contain chromatin-associated double-stranded DNA sequences, comprising the mutated form of HRAS. Large EVs may induce a stable transfection of the mutant form of HRAS into recipient wild type cells, resulting in increased proliferative capability and phenotypic abnormalities [49].

Angiogenesis and rearrangement of the tumor microenvironment are two further functions of large EVs that have been reported. Other components transported by large EVs such as tumor growth factor (TGF)-β vascular endothelial growth factor (VEGF), and microRNA (miRNA or miR)-1246, are known angiogenic agents. The TGF/SMAD signaling pathway is regulated by miR-1246, which induces endothelial cell proliferation and vessel sprouting. Recent study has discovered that Through EV-mediated transfer of the Vacuolar-ATPase subunit G1 and homeobox transcription factors, GBM organoids impact their adjacent environment, altering it toward a pro-tumorigenic state. Bertolini et

al. demonstrated that large EVs deliver these cargos to both neoplastic and non-neoplastic glial recipient cells, which could result in oncogenic reprogramming and activation of proliferation and motility pathways [51] [49]. In an in vitro prostate cancer (PCa) model, similar findings were revealed. Different cell types, such as normal prostate fibroblasts, have been reported to internalize large EVs in this environment. The level of -SMA, interleukin (IL)-6, and matrix metallopeptidase (MMP)-9 in stromal cells receiving PCa cell-derived large EVs increases, which has been linked to the development of a pro-tumorigenic microenvironment. The secretion of proteolytically active MMP-containing large EVs can promote amoeboid-type invasion of tumor cells. Furthermore, large EV-reprogrammed prostate fibroblasts might induce tumor growth in mice while stimulating endothelial tube formation in vitro. These investigations outlined the role of large EVs in the metastatic process through preparing cancer cells for detaching and spreading from the initial tumor bed. The involvement of large EVs in the interplay between tumor cells and the surrounding microenvironment, could be another topic of interest. The ability of vesicles shed by cancer-associated fibroblasts (CAF) to generate chemoresistance in either pancreatic or colorectal cancer models has recently been revealed in gastrointestinal tumors, demonstrating the bidirectionality of EVs transfer between tumor cells and tumor stroma. Intratumoral mesenchymal stem cells (MSC) can also release EVs that trigger gastric cancer cells to become resistant to 5-fluorouracil-induced apoptosis. These facts, on the other hand, mostly concern S-EVs, while the role of large EVs remains to be confirmed [49].

Moreover, large EVs are involved in cancer immune evasion. According to recent studies, large EVs produced from breast cancer (BC) can include high levels of indoleamine-2,3-dioxygenase (IDO), an enzyme involved in tryptophan metabolism that plays a key role in the formation of an immune-suppressed milieu by inhibiting T-cell proliferation. Consequently, cancer cells are presumed to use the large EV-mediated release of IDO to disseminate their suppressive signals throughout the tumor environment, however other mechanisms may also have a role. Leukocytes can also release large EVs, according to Nanou et al. [52] [49]. Other research has found that leukocyte-derived EVs play a key function in the control of the leukocyte-endothelial interaction, indicating that they may play a role in tumor progression by facilitating cancer cell intravasation and distribution to metastatic regions [49].

Large Oncosomes Functions and Internalization Mechanisms

Large oncosomes (LO) functional effects alters from straightforward proteolytic activity to the stimulation of pro-tumorigenic pathways in a variety of target cells, including other tumor cells and tumor microenvironment cells. LO can affect glutamine metabolism in PCa cells by stimulating GOT1, an enzyme that synthetize the production of glutamate from aspartate and α-ketoglutarate. LO released from an aggressive PCa cell line can increase both adhesion and invasion of PCa recipient cells through stimulating AKT by expressing the V-integrin on the LO surface. The cell migration augmentation has been shown through treatment with LO from LNCaP/MyrAkt1 cells, which contain an over-activated version of AKT [44]. Surprisingly, fibroblast that had been treated with LO also increased tumor cell migration. LO effect on tumor microenvironment has been

characterized for: stromal cells where LO treatment can increase the production of metastasis-related factors including brain-derived neurotrophic factor (BDNF), C-X-C motif chemokine 12 (CXCL12) and osteopontin. b) endothelial cells, in which LO promoted tube branching and whose migration was accelerated by LO isolated from the circulation of mice with metastatic disorder, c) normal fibroblasts (NAF) in which LO treatment increased the production of interleukin 6 (IL6), MMP 9, and α-smooth muscle actin (-SMA) promoting a provascularization phenotype through MYC activation. According to recent studies, by transferring the V-ATPase subunit V1G1 and the homeobox genes HOXA7, HOXA10, and POU3F2 to recipient cells through LO, glioblastoma neurospheres regulate their non-neoplastic environment [44].

An autocrine pathway (which is instinctively exclusive to tumor cells) and/or a paracrine mechanism (where both tumor cells and tumor microenvironment cells are involved) can be utilized by LO to perform all of the functions listed above [53] [54] [44]. Furthermore, it is critical to determine if the EVs docking event on the recipient cell is sufficient to activate a signaling cascade that results in functional changes and/or whether the EVs docking event is consistently followed by cargo release within the recipient cells. regarding to this, in recent studies, AKT activity has discovered to be crucial MYC-dependent stroma recipient cell conversion following PCa-derived LO absorption [55] [44]. Surprisingly, an active AKT in LO isolated from PCa cells and PCa patients' plasma has been discovered. Likewise, since αV-integrin on LO surface can affect tumor recipient cells through AKT activation, selective LO internalization cannot be excluded. However, it is still unclear if AKT activation in recipient cells was caused

by LO cargo release or was linked to endogenous AKT activation during LO docking/uptake. However, it's still unclear whether LO cargo release induced AKT activation in recipient cells or if it was correlated to endogenous AKT activation during LO docking/uptake [55] [35] [44].

Ciardiello et al. believe that all of LO's effect are most likely the result of both EV docking and membrane-membrane interaction, followed by large EV intake. Through phagocytosis, large particles internalization would be accomplished. Regarding to this phagocytosis, it is a type of endocytosis generally limited to specific phagocytes. Pinocytosis, on the other hand, is a cellular process that occurs in all cells and can effect on a variety of substances (i.e. Arf-6, flotillin-1-, CDC42- and RhoA). According to Minciacchi et al. study, the effective block of the pathway by Dynasore, a non-competitive inhibitor of the GTPase activity of dynamin, a protein essential for endocytosis and phagocytosis, but not by EIPA (5-(N-Ethyl-N-isopropyl) amiloride), a macropinocytosis blocker, reveals that LO internalization is similar to a phagocytosis-like mechanism [41] [44]. Nonetheless, it is still debatable whether the mechanisms of large EV uptake are identical to classic endocytosis pathways, such as receptor-dependent or fluid-phase endocytosis (a slow, non-specific process). Exosome experiments have indicated that changes in the cellular microenvironment (i.e. pH) can impact EV uptake. Additionally, studies show that EV uptake can be influenced by changes in the cellular microenvironment (such as pH).

Techniques for Large EVs' Isolation

1.Ultracentrifugation

Centrifugation for separation of particles is the traditional approach for EVs isolation. Cells, cell debris, apoptotic bodies, and biopolymer accumulation are firstly pelleted using low-speed centrifugation. After that, by resuspending the pellet and centrifuging it multiple times at high speeds the non-EV proteins are discarded. Many parameters influence the effectiveness of EV isolation by centrifugation, including sample viscosity, acceleration (g), and rotor type. Small EV isolation needs a high acceleration (100,000 g), whereas large EV isolation necessitates a lower acceleration. Many publications have found that consistent isolation can be achieved at 10,000 g, making large EV isolation easier [49]. While centrifugation is time-consuming, it requires a minimal number of chemicals and consumables and may be applied to relatively large initial quantities. Although it provides constant quantities of large EVs, they are usually contaminated by a variety of proteins, including albumin in plasma separated EVs or uromodulin/Tamm–Horsfall protein (THP) in urine vesicles. As a result, to validate the purity of collected vesicles sufficient controls are required, as inappropriate samples may impact downstream functional experiment results [49].

2.Ultrafiltration

Commercial membrane filters with pore diameters ranging from small to large is used in this method. All of the components larger than the holes are removed as the EV preparation passes through the membrane. Filters with large pore sizes eliminate large particles, while particles smaller than the target EVs are isolated from the filtrate later. Additional ultracentrifugation processes can be added, and results are conversely related to the number of filtering stages used, but directly correspond to the purity of the EV

preparations. The high pressure required during the filtration phases is a significant limitation of this approach, which could result in contaminant particle leakage or EV rupture [49].

3. Gel Filtration (Size Exclusion Chromatography)

Gel filtering is a technique for separating biopolymers that works by separating molecules depending on their hydrodynamic radius (such as polysaccharides, proteins, proteoglycans, etc.). EVs can be separated from plasma and urine protein complexes, and also lipoproteins, using this approach. A gel column is used to pass the EV solution through. Some samples reach the bottom of the column faster than others due to the gel's specific structure. EVs are separated from other components in this manner, allowing them to be eluted individually [49]. Various forms of columns are available for simple EV isolation using gel chromatography: Sepharose CL-4B (Sigma, St. Louis, MO, USA), Sepharose 2B (Sigma, St. Louis, MO, USA), qEV Size Exclusion Columns (Izon Science Ltd., Oxford, UK). The former approach is highly user-friendly, however, it would be costly. Even though using gel chromatography can result in great purity of EV preparations, the final particle concentration is usually diluted and can be quite low, needing further concentration procedures prior to subsequent utilization. Lastly, it’s important to bear in mind that no commercial kit currently exists that allows for the separation of different EV classes, rendering this method ineffective for the accurate isolation of large EVs [49].

4. Precipitation

Using of hydrophilic polymers to precipitate the EVs is the second most frequent method for EV isolation. The solubility of EVs is restricted by dispersing them in a solution of super hydrophilic polymers. Low-speed centrifugation (1500 g) can be used to precipitate the vesicles. Sodium acetate (for neutralizing negative charges on the EV membrane), polyethylene glycol, protamine (a positive charged molecule) or, the protein organic solvent precipitation (PROSPR) might all be utilized [49]. Despite the fact that this approach is significantly faster than ultracentrifugation, it usually results in the coprecipitation of non-EV nucleoproteins and proteins such as albumin and apolipoprotein E. It's typically employed when a large number of EVs are required but there's no need for extreme purity. Since this method cannot provide the separation of distinct EV classes, contamination by S-EVs should be considered when assessing large EVs isolated by precipitation [49].

5. EVs and Imaging Flow Cytometers

Nanoparticle flow cytometers have been created as a possible tool for detecting and analyzing molecules smaller than those measured by traditional cell cytometers. Imaging flow cytometers are another alternative for expanding the capabilities of flow cytometry. In addition to all of the diagnostic features of traditional cytometry (such as fast and high-throughput scatter measurement and a wide range of fluorescent markers), it also allows you to see images of the molecules being studied. It has a lower background noise and can differentiate actual single events by photographing objects and removing convergent events or detritus from the processing. However, imaging flow

cytometers, like nanoparticle flow cytometers, are not extensively used and require training to use [56] [57].

6. Immune Affinity Interaction

To selectively bind EVs, particular mAb directed against typical EV surface molecules including tetraspanins can be utilized in combination with magnetic beads. Highly porous monolithic silica microtips, plastic plates, and cellulose and membrane affinity filters are all suitable tools for similar aims. Magnetic beads covered with a pool of anti-CD9, anti-CD63, anti-CD81, and anti-EpCAM antibodies were used by some investigators to isolate EVs efficiently. EV-magnetic bead complexes are collected, then separated and rinsed using a magnet. This approach allows for faster isolation, higher EV purity, and harvesting of certain EV fractions, such as large EVs. This technique, on the other hand, is costly and has a low isolation efficacy, making large-scale processing difficult [49].

7. EV Markers for Quality Control

Quality controls are required following the extraction of large EVs from either cell culture supernatants or biological fluids to arrange EVs for downstream analysis. Flow cytometry and western blotting for protein composition evaluation, Tunable Resistive Pulse Sensing (TRPS) for dimensions measurement, and transmission electron microscopy (TEM) for morphological research are common assays used for this objective. The MISEV2018 provided the requirements for indicating the EV characteristics and purity [49]. At least a transmembrane protein linked with the plasma membrane and/or endosomes (such as tetraspanins, integrins, MHC-class I, etc.) and a

cytosolic protein commonly found in EVs (Flotillins, Caveolins, ALIX and ESCRT) are necessary. As cytochrome C, histones, and calnexin are not detected in S-EVs, numerous proteins related to non-compartments (including cytochrome C, histones, and calnexin) must be validated in large EVs. Finally, to confirm the parental source of these vesicles or demonstrate their functional activity, proteomics of the retrieved EVs should be investigated. To ensure the purity of EV preparations, non-EV co-isolated impurities including lipoproteins (APO1, fibronectin, collagen) for plasma and uromodulin for urine must be eliminated [49].

Large EVs and Autophagy

Secreted autophagosomes of the autophagy system, which carry distinct cargoes and have avoided lysosomal destruction and remain in the extracellular environment, are one mechanism that may be included in this heterogeneous population of exosomes and microvesicles [58]. Regarding the large EVs, Apoptotic bodies are formed during coordinated blebbing events corresponding to the controlled cell death mechanisms observed in apoptosis [59], whereas oncosomes are formed by cancerous cells blebbing off portions of the plasma membrane and frequently carry cargoes capable of increasing the malignancy of the original tumor site [32]. These larger EV subtypes are distinct to the phenomenon from which they are produced and to the disease state from which they are derived, notably in the case of oncosomes derived from various cancer tumor settings, where they may be useful as future oncogenic biomarkers. Autophagy is a physiological process found in cells throughout an organism that is both constitutive and inducible, with actions primarily focused on the generation of degradative substances and

intracellular quality control [60]. The molecular pathways that promote mammalian autophagy normally start when the cell is starved of amino acids or when mTOR is inhibited [61]. Following either of these processes, the ULK1 protein is activated, allowing the phosphorylation of Ser 14 on Beclin-1, which is now the primary autophagy activator protein [61]. Following interactions with phosphorylated Beclin-1, it will generate nucleation of the nascent phagophore by interacting with Vps34 and Vps15, as well as a variety of other proteins [62]. Following then, two different routes act in tandem to enhance the structure's elongation. One mechanism involves ATG4 cleaving the LC3 protein to produce LC3-I, which can then be conjugated to phosphatidylethanolamine (PE) by ATG3 and ATG7 to produce LC3-II, attaching the protein to the early phagophore [62]. The alternate pathway involves ATG12 binding to ATG5 via enzymatic activities with ATG7 and ATG10, after which ATG12 binds to ATG16L in an elaborate complex with the early phagophore structure [62]. These routes work together to finish the phagophore's elongation phase, which starts as a cup-shaped structure and ends as a closed-sphere autophagosome [33].

Evidences suggest that autophagy and endocytic pathways are intertwined in non-neuronal cells and neurons, and they share several common machineries. The fusion of LE/MVBs with autophagosomes produces amphisomes, which function as an intersection for these two pathways. The development of amphisomes which are an intermediate organelle with a diameter of 300-900 nm, is a critical phase in the maturation of autophagosomes prior to their final fusion with lysosomes for cargo destruction. Endosome biogenesis and maturation defects can affect amphisome production and, as a

result, autophagy activity. Autophagy or the fusion of autophagosomes with LEs/lysosomes has been demonstrated to be regulated directly by several endocytic regulators, such as Rab7 and ESCRTs, which are required for the proper function of the endocytic pathway. Amphisomes have been demonstrated to increase the secretion of mucus granules in goblet cells of the intestinal epithelium, which is needed for supplying the mucus barrier that defends against intestinal infections [63]. During secretory autophagy autophagosomes can fuse with late endosomes to create pre-lysosomal autophagic/ endocytic vacuoles called amphisomes [64]. Afterwards, the amphisomes merge with the plasma membrane, causing sequestered cargo such as dsDNA and histones to be released extracellularly, as well as intra-luminal vesicles (ILV) as exosomes [65]. Therefore, amphisomes formation is a necessary step in autophagosome maturation before they fuse with lysosomes to degrade cargo.

Taken together, amphisomes and other large EVs component are known to interact with recipient cells, where they have been reported to induce the development of numerous inflammatory mediators, which have been shown to harm and even death to organism exposed to them. For the purposes of a preliminary experiment, large EVs (2k) from T-cells and monocytes that have been infected with HIV-1, and large EVs from uninfected control cells will be used to look for the presence of viral protein. This study will explore the presence of virus in the large EVs and amphisome-like structures released from HIV-1 infected T-cells and myeloid cells, investigate that whether these viruses can infect the uninfected neighboring cells. Isolated large EVs from HIV-1 infected monocyte (U1) and T-cells (J1.1) will be employed as an experimental model for

this characterization, as viral proteins and RNAs identified may contribute to the development of inflammatory diseases. This understanding will hopefully be useful in the development of future medications and intervention options for people suffering from AIDS and other HIV-1-related inflammatory diseases.

MATERIAL AND METHODS

Cell Culture and Treatment

Jurkat (uninfected T cells), U937 (uninfected monocyte), J1.1 (HIV-1-infected T cells), U1 (HIV-1-infected monocyte) cells were cultured for seven days at 37 °C and 5.0 percent CO2 in full RPMI 1640 medium including 1 percent L-glutamine, 1 percent streptomycin/penicillin, and 10% exosome-free fetal bovine serum (FBS). Serum starvation (1% FBS) was used to synchronize the cells for three days (-72 hours). Cells were treated with cART. After that, the cells were washed and pelleted in 20% FBS media before being incubated with phytohemagglutinin (PHA; 10 g/L) and IL-2. After induction, samples were collected at 6, and 24 hours after release (+6 hours and +24 hours samples)

EV Isolation and Ultracentrifugation

The HIV-1 infected T-cell (J1.1), and myeloid (U1) cells were cultured in full RPMI medium in T75 flasks for two weeks before being synchronized by serum starvation as previously described. The cells were then washed and plated in 20 percent FBS media in two T25 flasks, one for 6 hours and the other for 24 hours, and PHA/IL-2 was used to induce T-cell (J1.1). The cells were centrifuged at 300 g for 10 minutes to pellet them, and the cell supernatant was collected. Dead cells and cell debris were pelleted using a further centrifugation at 2000 g for 45 minutes. The pellets were

resuspended in 50 L PBS after the supernatant was collected. At 4 °C, all centrifugations were carried out.

EV Capture with Nanotrap Particles

Nanotrap particles were used to isolate EV and virion from samples (Ceres Nanosciences, Inc.; Manassas, VA, USA). To prepare a slurry, equal volumes of each Nanotrap particle (NT80, NT82) were combined and resuspended in 1X PBS without calcium and magnesium. To trap EVs from supernatants, 60 µL of slurry were added to 1 mL of supernatant, and the samples were rotated overnight at 4 °C. The particles were resuspended (50 µL PBS for RNA isolation or 20 µL Laemmli buffer for western blotting) for subsequent experiments after being isolated and rinsed with PBS.

Virus Rescue Assay

The J1.1 and U1 supernatants from -72, +6, and +24 hours were used to treat naïve CEM and U937. A total of 10^6 naïve cells were resuspended in 30 µL supernatant and incubated for two days. Afterwards, 600 µL fresh complete RPMI1640 medium was added and the cells were allowed to incubate for two days. The cells were then harvested and pelleted for western blot analysis.

Preparation of Whole Cell Extracts and Western Blot Analysis

After cell centrifugation, they were washed with PBS. The pellet was resuspended in a lysis buffer containing 50 mM Tris-HCl (pH 7.5), 120 mM NaCl, 5 mM EDTA, 0.5 percent Nonidet P-40, 50 mM NaF, 0.2 mM Na3VO4, 1 mM dithiothreitol (DTT), and 1 complete protease inhibitor cocktail tablet per 50 mL (Roche Applied Science, Mannheim, Germany). The mixture was vortexed every 5 minutes for 25 minutes on ice.

Cell debris was separated using a 12,000 g centrifuge at 4 °C for 10 minutes. According to the manufacturer's instructions, the protein concentration was determined using the Bradford test (Bio-Rad, Hercules, CA, USA).

The samples were combined and heated with Laemmli buffer for western blot analysis. Each sample was put onto a 4–20 percent Tris/glycine 1.0 mm gel in 15–20 microliters (Invitrogen, Carlsbad, CA, USA). The samples were processed at 160 V for an hour before being transferred at 50 mA on PVDF membranes (Millipore, Burlington, MA, USA). The membranes were blocked in PBS-T (PBS with 0.1 percent Tween-20) for 30 minutes at 4 °C before being incubated with the corresponding primary antibody against the proteins of interest overnight at 4 °C in PBS-T. The membranes were rinsed the next day and incubated for 2 hours at 4 degrees Celsius with the proper HRP-conjugated secondary antibody. Clarity western increased chemiluminescence (ECL) Substrate (Bio-Rad, Hercules, CA, USA) was used to activate HRP luminescence, which was then photographed using a ChemiDoc Touch system (Bio-Rad, Hercules, CA, USA).

RNA Isolation and RT-qPCR

Total RNA was extracted from cell pellets and EV-enriched NT80/82 pellets for quantitative analysis of HIV-1 RNA. Trizol Reagent (Invitrogen, Carlsbad, CA, USA) was used to isolate RNA according to the manufacturer's instructions. A GoScript Reverse Transcription System (Promega, Madison, WI, USA) was used to synthesize cDNA from total RNA using specified reverse primers. HIV-1 Gag Reverse (5′-GCT GGT AGG GCT ATA CAT TCT TAC-3′, Tm = 54 °C), HIV-1 TAR Reverse (5′-CAA CAG ACG GGC ACA CAC TAC-3′, Tm = 58 °C), and HIV-1 Envelope Reverse (5′-

TGG GAT AAG GGT CTG AAA CG-3′; Tm = 58 °C). TAR Reverse (5′-CAA CAG ACG GGC ACA CAC TAC-3′, Tm = 58 °C) and TAR Forward (5′-GGT CTC TCT GGT TAG ACC AGA TCT G-3′, Tm = 60 °C) primers were used to perform RT-qPCR on the produced cDNA samples. As discussed before [3], DNA serial dilutions from HIV-1-infected 8E5 cells were applied as standards.

Nanoparticle Tracking Analysis

The ZetaView® Z-NTA (Particle Metrix) software was used to perform nanotracking analysis for EV measurement and size (ZetaView 8.04.02). Prior to taking sample readings, calibration was done with 100 nm polystyrene nanostandard particles (Applied Microspheres) at a sensitivity of 65 and a minimum brightness of 20. For each reading, the instrument parameters were set as previously described [3] In three independent reads, 1 mL of material diluted in DI water was put into the cell, followed by measurements of particle size and concentration at 11 unique locations across the cell. The machine software computed the mode diameter size and the sample concentration after automated analysis and the removal of any outliers. The Zeta View measurement data was evaluated with the manufacturer's software, and raw data was plotted with Microsoft Excel 2016. In our data, we show the particle size distribution.

Size Exclusion Chromatography (SEC) Using qEV Columns

J1.1 and U1 were centrifuged for 45 minutes at 2000g to pellet 2k EVs, then washed with PBS by adding 30 mL PBS and centrifuge for 45 minutes at 2000g to remove any cells or large particles. In both times, the temperature was 4 ° C. Equilibrate the column and sample buffer at temperatures between 18 and 24 ° C. Izon column were

used in this study (qEV1/35 nm & qEV1/70 nm). At least one column volume of sample buffer was used to flush the column (3.5 mL of PBS without Mg and Ca). Buffer was flowed through the column until all of the buffer reached loading frit, at which point the column will stop flowing. The loading frit was filled with the volume of the prepared centrifuged samples. The void volume was accumulated right away (1mL of void volume). 200 µL of the sample was entered the loading frit, the column was toped up with buffer; after the void volume has been collected, 1-40 fractions of samples with 200 µL in each tube were collected. After collecting all 40 tubes, each of the five fractions were combined, and finally the 8 fractions which each contained 1000 µL of samples were ready to use.

Immunoprecipitation

For immunoprecipitation, 500 µL of fractionated samples (1-5 fraction), along with 3 µg (15 µL of working solution with the concentration of 200 µg/mL) of Lamp1 primary antibody had been rotated overnight at 4°C. 500 µL samples with IgG were also included. 30 µL of protein A and protein G magnetic beads (Thermo-Fisher Scientific) were added into each IP samples the next day. This mixture was rotated at 4°C for at least 2 hours. Magnetic precipitation of beads was performed and then samples were washed twice with 500 µL of PBS + 0.001% of Tween-20.

Statistical Analysis

Using Microsoft Excel, standard deviations (S.D.) were calculated for each quantitative experiment. P-values were determined using a two-tailed student's t-test,

with $p < 0.05$ indicating statistical significance, $p < 0.01$ indicating larger significance, and $p < 0.001$ indicating maximum significance.

RESULT

Distinct Extracellular Vesicle Populations Can Be Separated by Centrifugation

Previous investigations have generated a method that has become a standardized process within our laboratory for the separation, isolation, and purification of extracellular vesicle population from HIV-1 infected human cells (**Fig. 1**). This approach has been demonstrated to be successful in isolating extracellular vesicle populations from media containing cell supernatant. In a nutshell, the procedure entailed culturing a volume of HIV-1 infected T-cells and monocytes for five days, then separating the supernatant from the cell pellet. To separate the cells from the supernatant, the cell-containing media was spun at 300 g for 10 minutes after it was established that the cells had attained an adequate level of confluence. After that, the supernatant was centrifuged for 45 minutes at 2000 g (2K). The pellet was then isolated with a PBS wash and consolidated into a single 1.5 ml tube. Large EVs in the 2K separation obtain from this method, which are separated by density. Although no filters were employed on any of the processed material in this experiment, this procedure has proven effective in prior experiments [2] in our lab for dedicated exosome isolation and analysis.

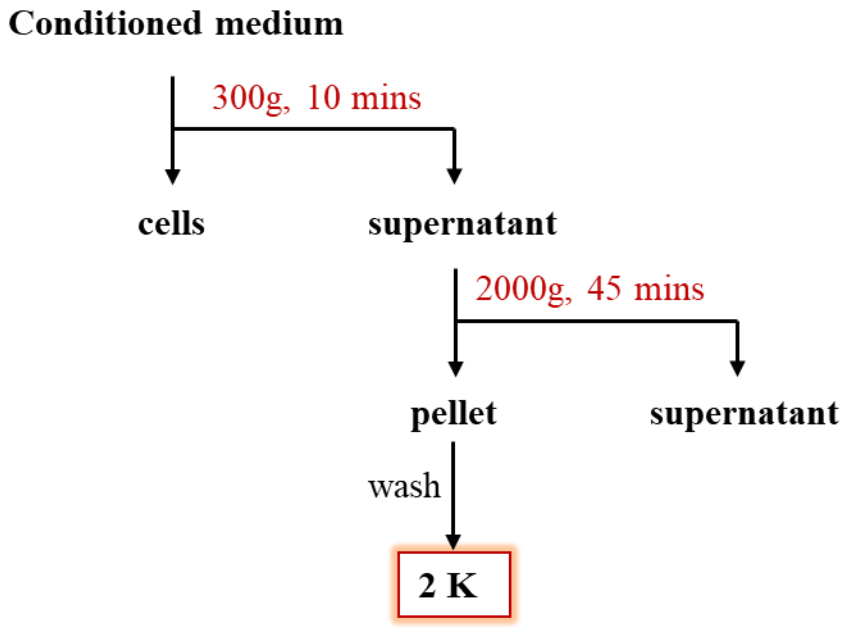

Figure 1. Centrifugation Workflow for Separating Large Extracellular Vesicles. Centrifugation on supernatants for 45 minutes with 2000 g generates pellets comprising large EVs/apoptotic, enabling for the successful separation of EVs from unprocessed supernatants into large EV populations. EVs are separated by density in this method.

Purification of Large EVs Released by HIV-1 Infected Cells Through Size Exclusion Chromatography

HIV-1 infected J1.1 were synchronized in G0 phase by serum starvation in 1% FBS RPMI for 72 hours. Afterward, cells were released in serum-rich media containing 20% serum, and inducers including IL-2, and PHA to initiate viral transcription and resume normal cell cycle. The supernatant sample was collected at 24 hours after release (+24 hours). Sample was spun at 300 g for 10 minutes to separate cells from supernatant. Next, the supernatant was centrifugated at 2000 g for 45 minutes to obtain large EVs in the 2K separation. The pellet then has been resuspended in 500 ul of PBS and

centrifugated at 2000 g for 45 minutes in order to be washed. In the next step, we performed size-exclusion chromatography of the 2K supernatant and purified samples through Izon columns precipitation. As particles move through columns packed with porous polysaccharide resin, they are separated by size. The size of the particles will determine how they are dispersed among the fractions, with the largest particles exiting the column first and the smallest particles exiting the column last. In the first step, two sizes of column were used (35 nm and 70 nm). which the 35 nm column purified the samples with optimum recovery range between 35 to 350 nm, and the 70 nm column purified the samples with optimum range between 70 to 1000 nm. After 2K EVs entered the column, 1 mL of void volume, which is the volume of mobile phase needed to elute a molecule from the stationary phase with no retention, were collected. Afterward, 40 fractions of the 2K samples were collected. Then we combined every 5 fractions. As a result of this purification, finally, 8 fractions of samples were collected which the first fraction (1-5) were the heaviest and largest particles (**Fig. 2**).

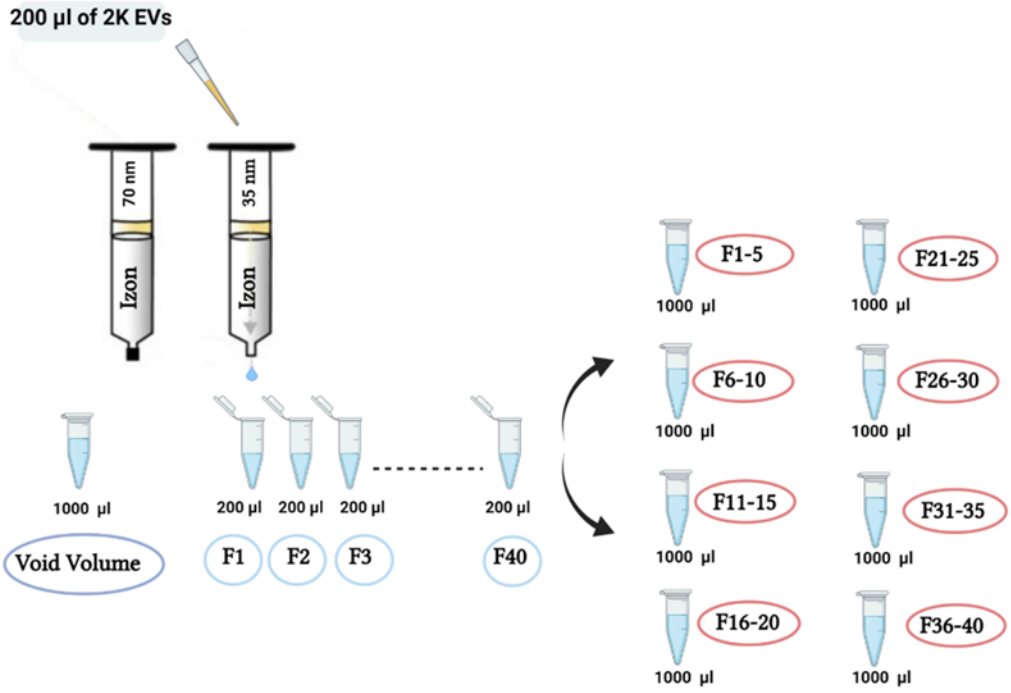

Figure 2. Purification of Large Extracellular Vesicles (2K) Through Izon column Size Exclusion Chromatography. Size exclusion chromatography columns separate particles based on their size. 200 µL of J1.1 sample was entered into Izon column. after the 1000 µL of void volume has been collected, 1-40 fractions of samples with 200 µL in each tube were collected. After collecting all 40 tubes, each of the five fractions were combined, and finally the 8 fractions were ready to use.

Characterization of Fractionated Large Extracellular Vesicles (2K)

Following of this chromatography, we performed western blot with 8 fractions of samples and probed for the presence of viral protein p24, and the proteins supposed to express on the amphisomes surface such as LC3, Rab5 and Lamp1. The results show that in 35 nm column, p24 was detected in the first fraction, which is the heaviest and largest fraction, but nothing special about other markers was found (**Fig. 3A**). On the other hand, in 70 nm column, beside the expression of p24 in the first fraction, we can also see the expression of Rab5 in the largest fraction (fraction 1-5) (**Fig. 3B**). Taken together this data show that viral protein and Rab5, as an amphisome marker in this study, are accumulated in the heaviest fraction and larger particles but not in the smallest one. Moreover, using 70 nm Izon column could provide more reliable data for this study; As a result, for further purification, the 70 nm Izon column has been used for size exclusion chromatography.

A)

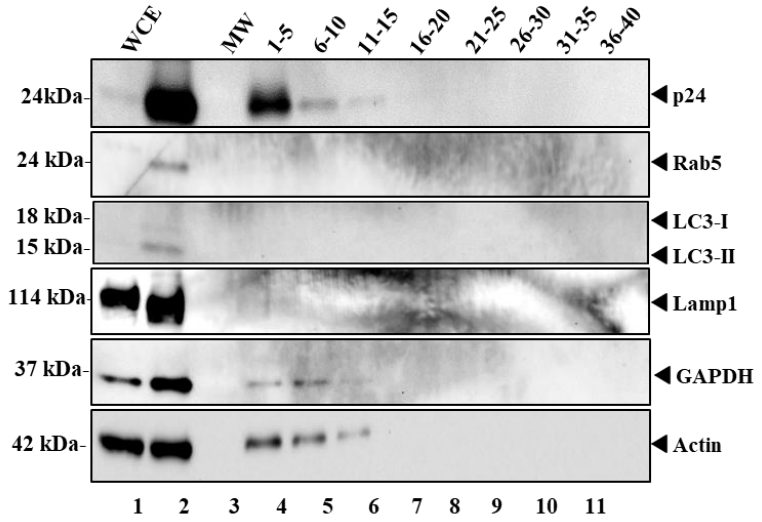

B)

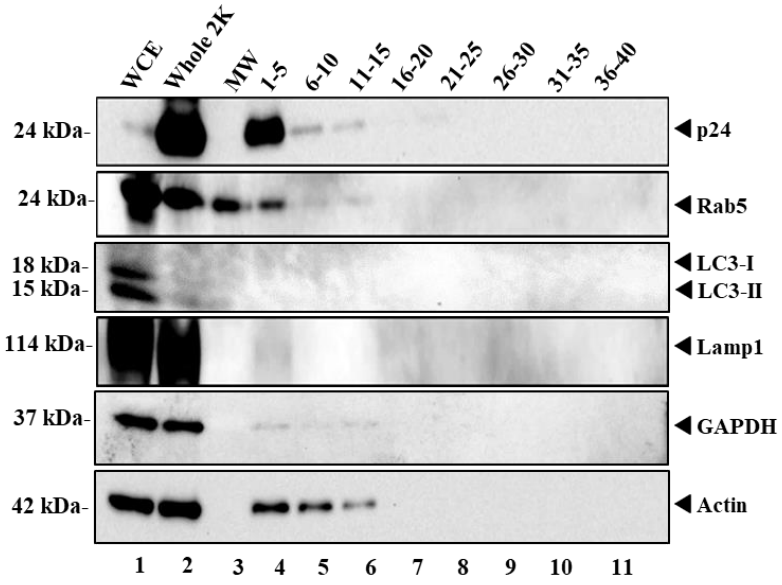

Figure 3. Characterization of Large EVs Released by HIV-1 Infected Cells

Western blot analysis of size exclusion chromatography of HIV-1 infected T-cell (J1.1) released at +24 hours. The samples were purified through 2 different sizes of Izon column. Data from 35 nm Izon column demonstrating the presence of viral protein in the fraction1-5 which is the largest fraction. Other proteins have been not expressed in any fractions (**Fig. 3A**). In the 70 nm column, p24 again is strongly expressed in the largest fraction. We also have the expression of Rab5 in the largest fraction (**Fig. 3B**)

Fractionated Large EVs Produced by Infected T-cells and Monocyte Contain Viral RNA

After performing western blot for fractionated large EVs released by HIV-1 infected T-cell (J1.1), we isolated the RNA of the first (1-5), middle (16-20) and the last (36-40) fractions of each Izon column samples and performed RT-qPCRed for the presence of TAR, TAR-*gag* and *env* transcripts. The data shows that the first fraction (1-5) of 35 nm column samples contain the highest level of viral RNA which significantly decreased in the smallest fractions (16-20 and 36-40) (**Fig. 3A**). We can also see the presence of all three viral RNA in the first fraction (1-5) of 70 nm column samples (**Fig. 3B**). Collectively, these finding show the presence of viral RNA in the largest particles of large EVs released from HIV- infected T-cells.

A)

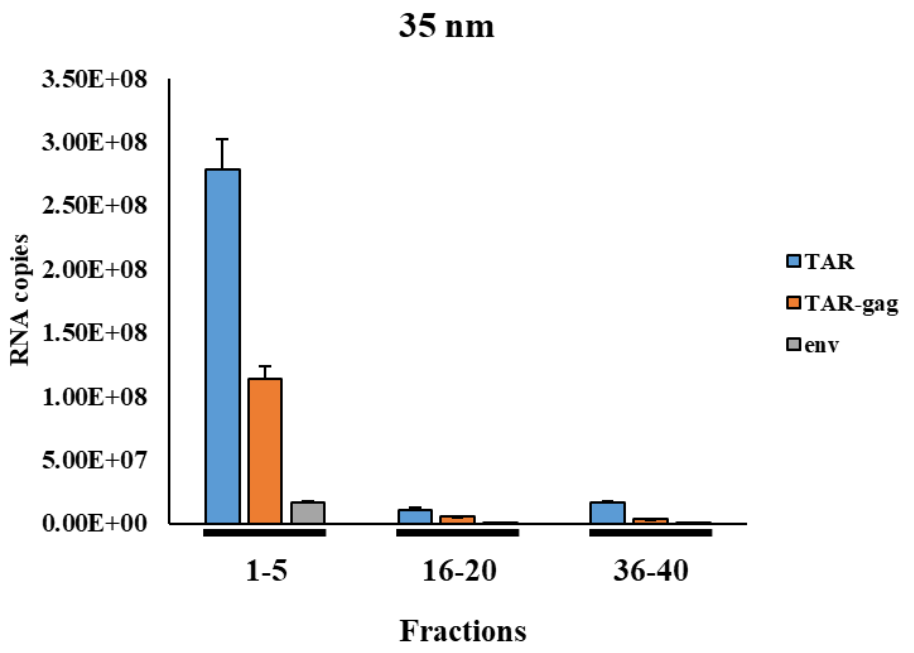
35 nm
3.50E+08
3.00E+08
2.50E+08
2.00E+08
1.50E+08
1.00E+08
5.00E+07
0.00E+00
RNA copies
1-5
16-20
36-40
Fractions
TAR
TAR-gag
env

B)

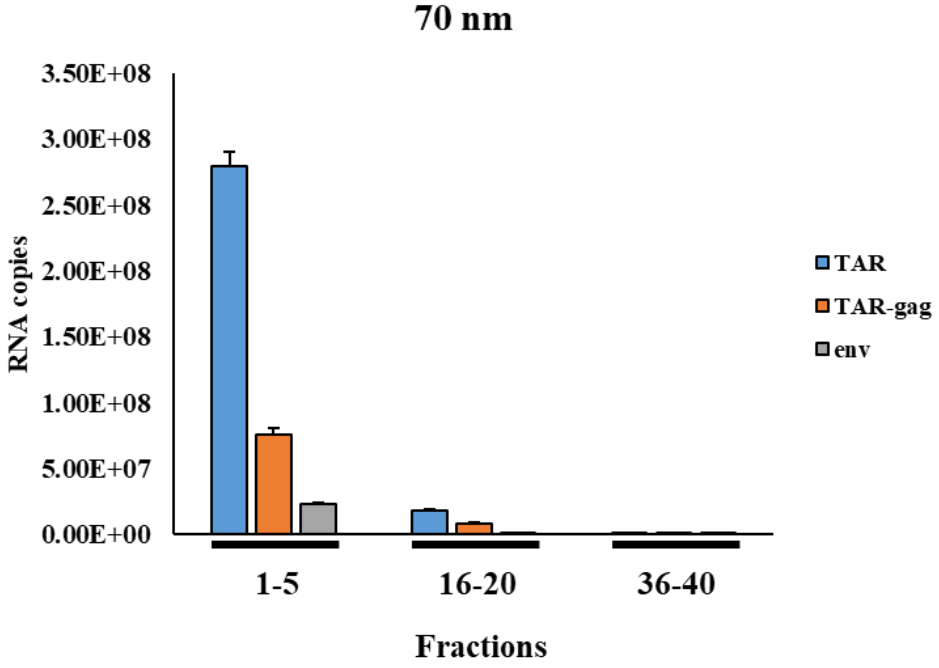
70 nm
3.50E+08
3.00E+08
2.50E+08
2.00E+08
1.50E+08
1.00E+08
5.00E+07
0.00E+00
RNA copies
1-5
16-20
36-40
Fractions
TAR
TAR-gag
env

Figure 4. The Presence of Viral RNA in The Larger Particles of Large EVs Released by HIV-1 Infected T-cell. HIV-1 viral RNA transcripts, TAR, TAR-*gag* and *env* are accumulated at the highest level in the larger fraction (1-5) of 2K EVs which purified through 35 nm size exclusion chromatography Izon column. The level of RNA significantly decreased in the other fractions (16-20 & 36-40) which are the smallest one (**Fig. 4A**). Data from 70 nm Izon column again show the highest level of viral RNA in the first fraction which dramatically decreased in the smallest fractions (**Fig. 4B**).

Characterization of EVs and Virions Released by HIV-1-Infected Cells Over Time

In our pervious study, we investigated to grasp whether EVs are released before virions, if both are released at the same time, or if virions are released first. To better control of EVs and virion release, we synchronized all uninfected and infected HIV-1 T-cells at G0 by adding serum starvation medium containing 1% serum, and then released them using complete medium containing 20% serum, IL-2, and PHA to reverse latency and activate HIV-1 transcription. We collected the supernatant at 0, 3, 6, 12, and 24 h post-release timepoints and added NT80/82/86 nanoparticles to enrich EVs and viruses and prepared them for downstream assays [5]. Data shows that EV markers such CD63 and CD9 were present 3 hours after release, and that CD63 levels increased in HIV-1-infected cells for up to 24 hours. There was also an increase in CD9 and the CD81 markers in the infected cells. These findings suggest that the expression and release of tetraspanin family members (CD63, CD9, and CD81) may be changed in infected cells. Then we looked at autophagy markers such as p62 and LC3-I/II family members. These markers show how autophagosomes form and whether or not they are secreted from infected cells. Starting at 6 hours after release, the HIV-1-infected cells released more p62 and LC3-I/II, as expected. Finally, we probed for the presence of viral proteins such

as gp120, Nef, p24, and Pr55 (Gag precursor of p24). Western blot analysis revealed the presence of all proteins starting at 6 hours and increasing up to 24 hours. These findings show that EV markers are present before viral markers and which increase over time up to 24 hours after G0 release (**Fig. 5**).

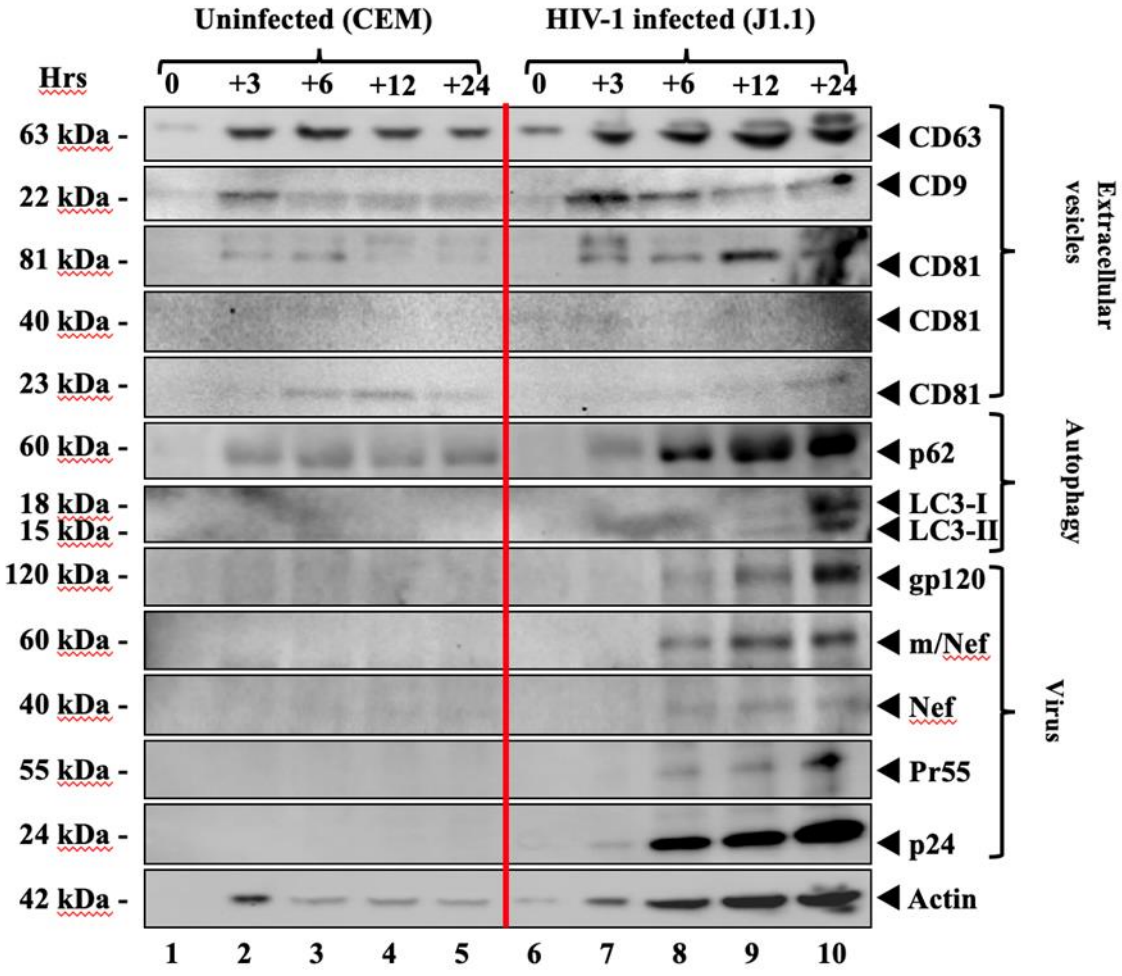

Figure 5. Characterization of EVs and Virions Released by HIV-1-Infected Cells Over Time. CD63 and CD9 were present 3 hours after release; CD63 levels increased in HIV-1-infected cells for up to 24 hours. The level of CD9 and the CD81 markers expression in the infected cells were increased which suggest the expression of tetraspanin family members (CD63, CD9, and CD81) may be changed during infection. Autophagy markers, p62 and LC3-I/II expression started at 6 hours in HIV-1 infected cells. gp120, Nef, p24, and Pr55 viral proteins started to release at 6 hours and increased up to 24 hours. Collectively these data show that EV markers are present before viral markers and which increase over time up to 24 hours after G0 release [5].

Enhanced Levels of Extracellular Viral RNA Post-Release

We used RT-qPCR to detect the presence of the TAR, TAR-*gag*, and *env* transcripts in RNA extracted from extracellular environment. Data depicts the presence of all three transcripts at 3 hours, but there is a dramatic increase in all three populations up to 24 hours. The TAR levels were increased the highest, as expected, since this reflects basal transcription before full-length genomic RNA synthesis (**Fig. 6**). Collectively, these findings suggest that, similar to viral protein accumulation in the extracellular environment, all three types of RNA accumulated over time in the induced releasing cells.

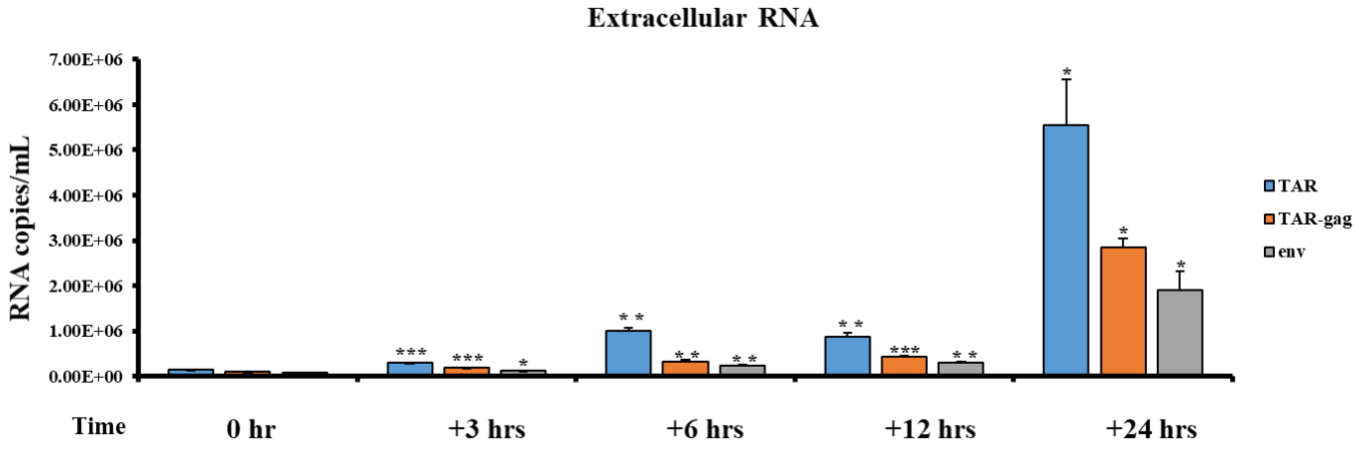

Figure 6. Levels of Viral RNA Content of Secreted EVs and Virions from HIV-1 Infected Cells. Data from RT-qPCR show the presence of all three viral transcripts (TAR, TAR-*gag* and *env*) at 3 hours, but a dramatic increase in all three populations at 24 hours fraction. The TAR levels were increased the highest, as expected, since this reflects basal transcription before full-length genomic RNA synthesis.

HIV-1 RNA Content of Large EVs Produced by Infected T-cells and Monocyte

Here we performed RT-qPCR to find out the presence of viral RNA in large EVs (2K) collected from three fractions, prior to release (-72 hours), early released (+6 hours) and post released (+24 hours) of HIV-1 infected T-cell (J1.1) and myeloid cell (U1). By serum starvation in 1% FBS RPMI for 72 hours, HIV-1 infected J1.1 and U1 were synchronized in the G0 phase. Following that, cells were placed into serum-rich media containing 20% serum. Inducers such as IL-2 and PHA were added to T-cell (J1.1) to start viral transcription and return to normal cell cycle. At 24 hours following release, a sample of supernatant was collected. Separating cells from supernatant requires ten minutes of spinning at 300 g. To obtain big EVs in the 2K separation, the supernatant was centrifugated at 2000 g for 45 minutes. After that, the pellet was washed by resuspending it in 500 ul of PBS and centrifuging it at 2000 g for 45 minutes. Then, we isolated RNA from samples and performed RT-qPCR for the presence of TAR, TAR-*gag* and *env* transcripts. Data shows presence of all three transcripts at -72 hours, +6 hours and +24 hours in both J1.1 large EVs. However, the level of RNA at -72 hours and +24 hours samples are higher than +6 hours one (**Fig. 7A**). All three fractions of U1 large EVs

samples also contain viral RNA which the level of RNA increases over time up to 24 hours (**Fig. 7B**) Collectively, these finding suggest that, similarly to presence of viral protein in the extracellular environment, there was an accumulation of all three classes of viral RNA in the induced released EVs.

A)

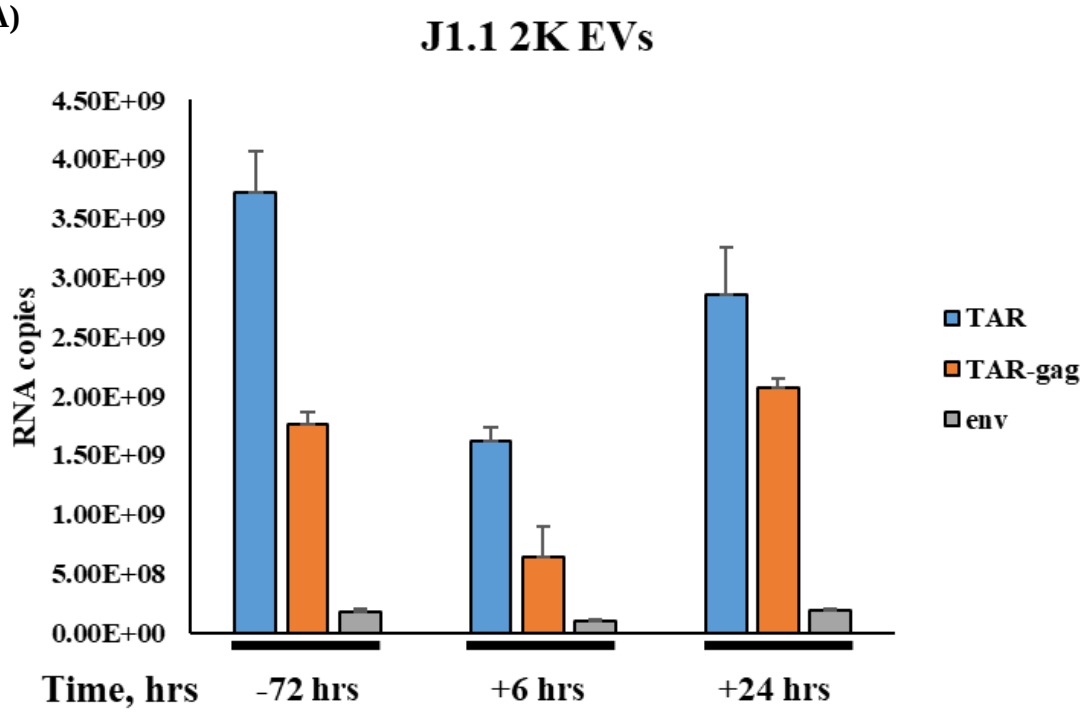

B)

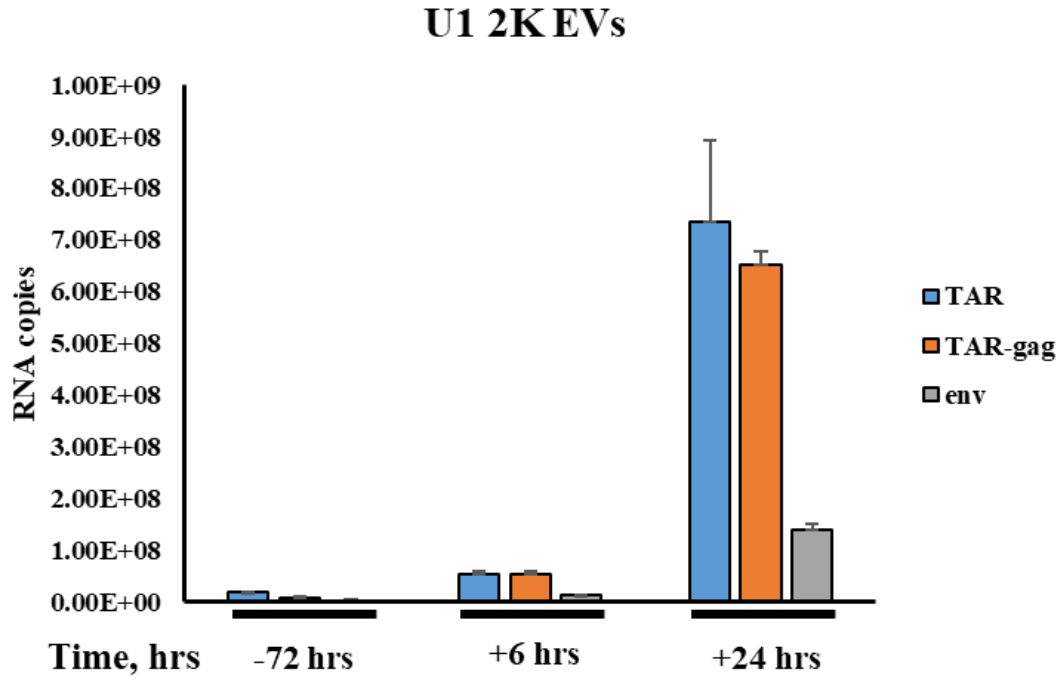

Figure 7. The Presence of Viral RNA Content of Secreted Large EVs from HIV-1-infected cells. RT-qPCR data shows that all three fractions, -72hours, 6 hours, and 24 hours, of Large EVs released by HIV-1 infected J1.1 contain TAR, TAR-*gag* and *env* viral RNA. However, the level of viral RNA in +6 hours is less than -72 and +24 hours EVs (**Fig. 7A**). HIV-1 infected U1 data shows the presence of viral RNA in all three fractions (-72, +6 and +24 hours) which the level of that increases over time and reaches to the highest level at +24 hours (**Fig. 7B**).

Functional HIV-1 Virus Rescue of Large Fractions Released by HIV-1 Infected Cells

Here, we asked whether large EVs from prior to release (-72 hours), early released (+6 hours), and post released (+24 hours) contained functional viral particles. to achieve this goal, we performed virus rescue assay and incubated all three fractions of samples with uninfected T-cell line (CEM) and myeloid cell line (U937) for 48 hours at 37 °C. Following potential infection from the -72, +6, and +24 hours samples, the cells

were pelleted, washed, lysed, and ran on a 4–20% SDS-PAGE followed by western blotting with an anti-gp120, Nef, and p24 antibodies. Data from J1.1 2K EVs shows that previously uninfected cells treated by large EV samples from -72- and +24-hours fractions produced viral proteins, but the ones treated with -6 hours fraction did not (**Fig. 8A**). U1 2K samples also demonstrates the presence of viral protein in -72- and +24-hours fractions (**Fig. 8B**). Taken together, these data demonstrate that although the +6 hours fraction contain viral proteins and RNA, it was found not to be infectious. On the other hand, both J1.1 and U1 2K EVs at -72- and +24-hours fractions contain fully-fledged virion and are infectious.

A)

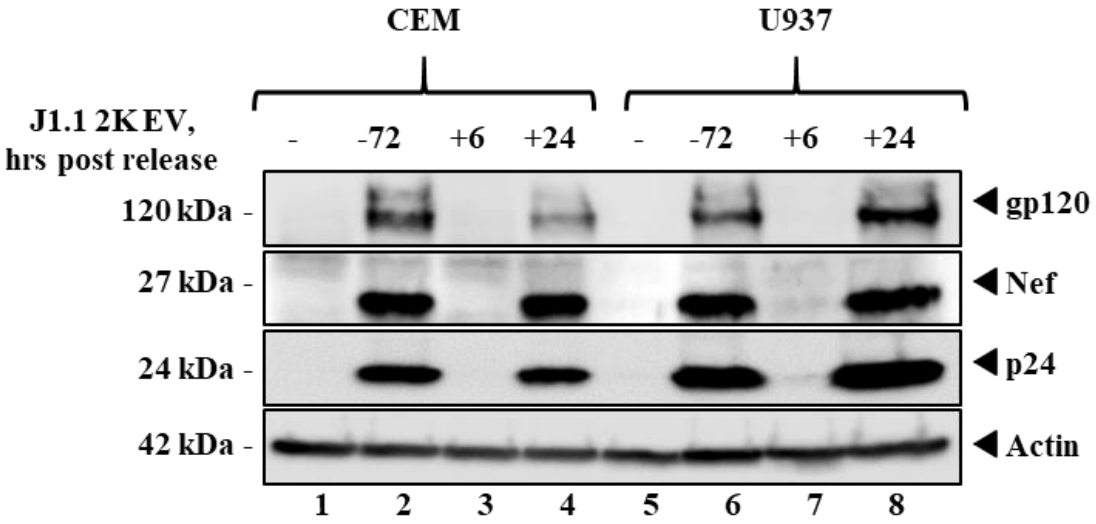

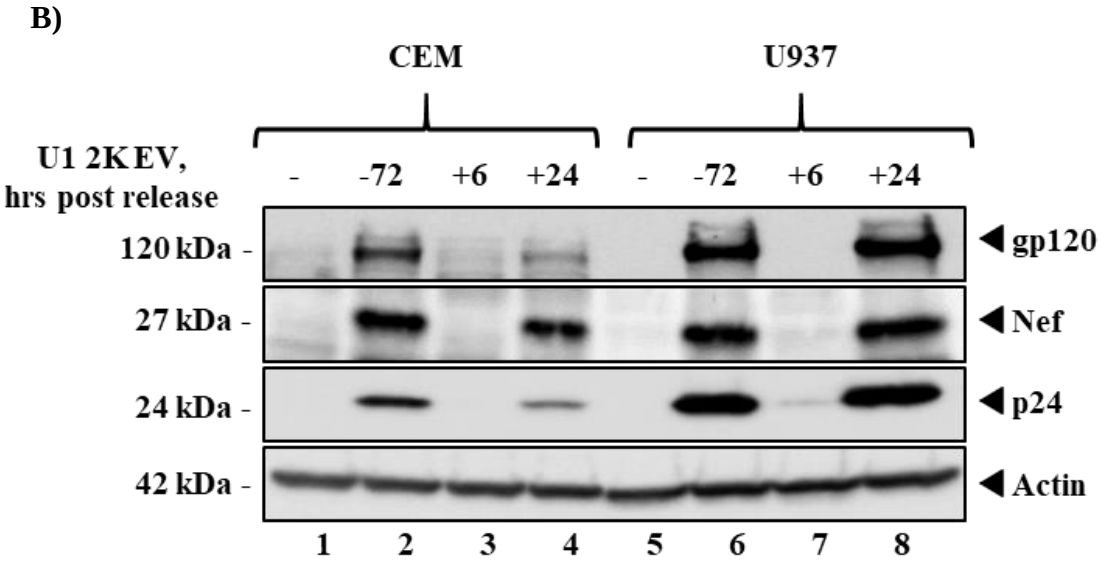

Figure 8. Infectivity Assay of The Large Fractions Released by HIV-1 Infected T-Cells and Myeloid Cells. Uninfected T-cell and monocyte were treated with HIV-1 infected large EVs. Western blot analyses then performed to probe for viral proteins. Data from J1.1 2K EVs shows that previously uninfected cells treated by large EV samples from -72- and +24-hours fractions produced viral proteins, but the ones treated with -6 hours fraction did not (**Fig. 8A**). U1 2K samples also demonstrates the presence of viral protein in -72- and +24-hours fractions. As a result, the +6 hours fraction was found not to be infectious (**Fig. 8B**).

Large Extracellular Vesicles Expressing Lamp1 on The Surface Are Infectious

Here we decided to investigate more specifically the infectivity of the large EVs at prior to release fraction (-72 hours) which express lamp1 protein on the surface. Since the Lamp1 is expressed on the surface of amphisome-like organelle, as previously mentioned, in this study we considered this protein as an amphisome marker. First of all, we performed immunoprecipitation of Lamp1 antibody, by using Lamp1 antibody along with IgG antibody as a negative control. After adding antibodies of interest, the samples had been rotated overnight at 4°C. then protein A&G magnetic beads were added into

each IP samples the next day. This mixture was rotated at 4°C for at least 2 hours. Magnetic precipitation of beads was performed and then samples were washed twice with PBS + 0.001% of Tween-20. After harvesting the Lamp1 positive particles, we applied virus rescue assay through infection of two cell types. We incubated prior to released, -72 hours samples, with uninfected T-cell line (CEM) and myeloid cell line (U937) for 48 hours at 37 °C. Following potential infection from the -72 hours samples, the cells were pelleted, washed, lysed, and ran on a 4–20% SDS-PAGE followed by western blotting with an anti-p24 antibody. Data shows the expression of p24 in the previously uninfected T-cells and myeloid treated by Lamp1-positive 2K EVs secreted from J1.1 (**Fig. 9A**). p24 was also expressed in both CEM and U937 treated by Lamp1-positive 2K EVs released by U1 (**Fig. 9B**). Densitometry count was used to measure the level of p24 expression (**Fig. 9C-D**). Collectively, these data indicate that the large 2K EVs at prior to release fraction (-72 hours), which express Lamp1 on the surface are infectious.

A)

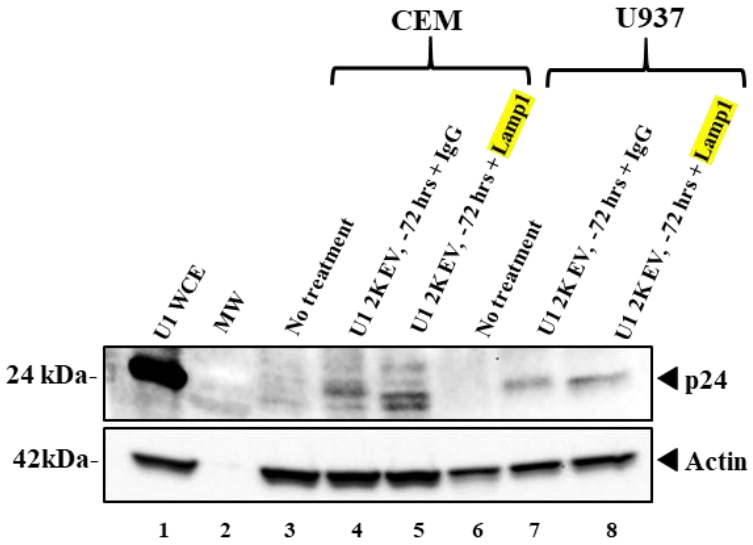
CEM
U937
U1 WCE
MW
No treatment
U1 2K EV, -72 hrs + IgG
U1 2K EV, -72 hrs + Lamp1
No treatment
U1 2K EV, -72 hrs + IgG
U1 2K EV, -72 hrs + Lamp1
24 kDa-
p24
42kDa-
Actin
1 2 3 4 5 6 7 8

B)

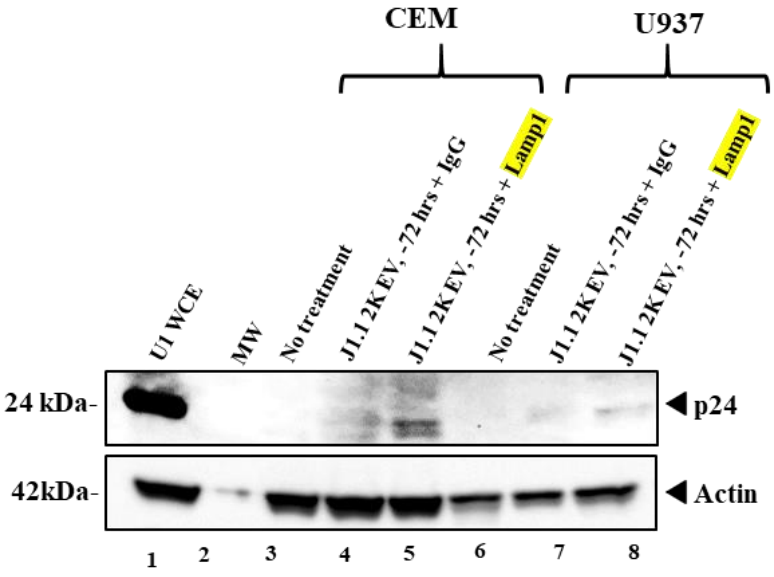
CEM
U937
U1 WCE
MW
No treatment
J1.1 2K EV, -72 hrs + IgG
J1.1 2K EV, -72 hrs + Lamp1
No treatment
J1.1 2K EV, -72 hrs + IgG
J1.1 2K EV, -72 hrs + Lamp1
24 kDa-
p24
42kDa-
Actin
1 2 3 4 5 6 7 8

C)

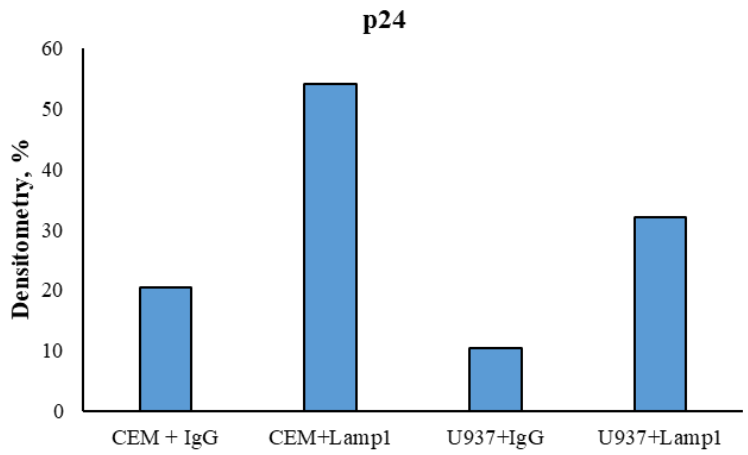

D)

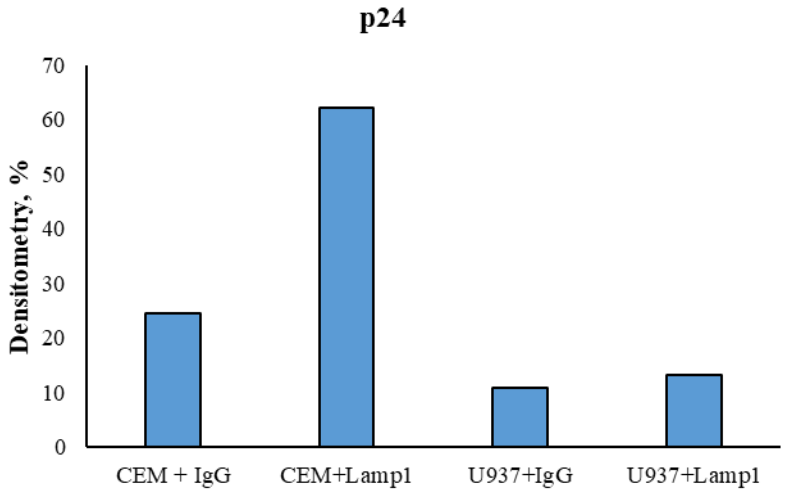

Figure 9. HIV-1 Virus Rescue of Large Particles Expressing Lamp1 on The Surface.
Western blot data shows the expression of p24 in the previously uninfected T-cells and myeloid treated by Lamp1-positive 2K EVs secreted from J1.1 (**Fig. 9A**). p24 was also expressed in both CEM and U937 treated by Lamp1-positive 2K EVs released by U1 (**Fig. 9B**). Densitometry count was used to measure the level of p24 expression (**Fig. 9C-D**).

DISCUSSSION

In reviewing the recent literature, viral proteins and RNAs are carried by extracellular vesicles, including exosomes from virally infected cells, which are taken up by naive cells and modify their function. Our pervious works revealed that exosomes from HIV-1-infected cells transmitted viral RNAs and proteins to nearby cells, resulting in either stimulation or negative consequences [66] [67]. EVs were also discovered to ready the environment for viral propagation. As a result, one cannot deny is the understanding the dynamics of EV and virus release in a timely manner. Here, in this study, the component and population of Large EV released by virally infected cells were investigated.

Additionally, along with large EVs characterization, we investigated the other large vesicles produced through secretory autophagy which called secretory amphisomes. Amphisomes are cellular degradative organelles. However, multiple investigations have shown that secretory amphisomes, a non-degradative amphisome population, may represent an unconventional secretion mechanism involving autophagy-dependent fusion with the plasma membrane. Amphisomes were found to increase the release of mucus granules in goblet cells of the intestinal epithelium, which is necessary for forming the mucus barrier that defends against intestinal infections [63]. As previously in this study mentioned, amphisomes which are produced through the fusion of LE/MVBs with

autophagosome during autophagy pathway, function as an intersection between degradative and secretory autophagy. As a results, the formation of amphisomes, these intermediate/hybrid organelle with a diameter of 300-900 nm, is a crucial phase in the maturation of autophagosomes prior to their final fusion with lysosomes for cargo destruction. During secretory autophagy autophagosomes can fuse with late endosomes to create pre-lysosomal autophagic/ endocytic vacuoles called amphisomes [64]. Afterwards, the amphisomes merge with the plasma membrane, causing sequestered cargo such as dsDNA and histones to be released extracellularly, as well as intra-luminal vesicles (ILV) as exosomes (**Fig. 10**) [65]. Since, amphisomes and other large EVs content can interact with recipient cell and transfer their biological cargo, they have been reported to induce the development of numerous inflammatory mediators, which have been shown to harm and even death to organism exposed to them. Studies show that several proteins are expressing on the surface of the amphisome which are including Lamp, Rab7, Rab5, LC3, EEA1 and p22phox protein [68] (**Fig. 11**). Lamp1 or lysosomal associated membrane protein1 involves in lysosome fusion with endosome and protect the lysosomal membrane against hydrolyze enzyme. On the other hand, Rab7 plays an important role in the fusion of phagosomes with lysosome; the fusion of early endosomes with endocytic vesicles, as well as early endosomes motility is regulated by Rab5. LC3 is required for autophagosome formation and maturation, as well as serving as an autophagy adapter protein. Early endosome antigen1 or EEA1 is restricted to the early endosome and plays an essential role in trafficking, and finally p22phox protein is a principal content of the membrane-bound oxidase of phagocytes which produces

superoxidase; collaborates with NOX3 to form NADPH oxidase producing superoxidase. In this study we characterized amphisomes along with large EVs to better understand the role of these organelle on the enhancement of HIV-1 infection.

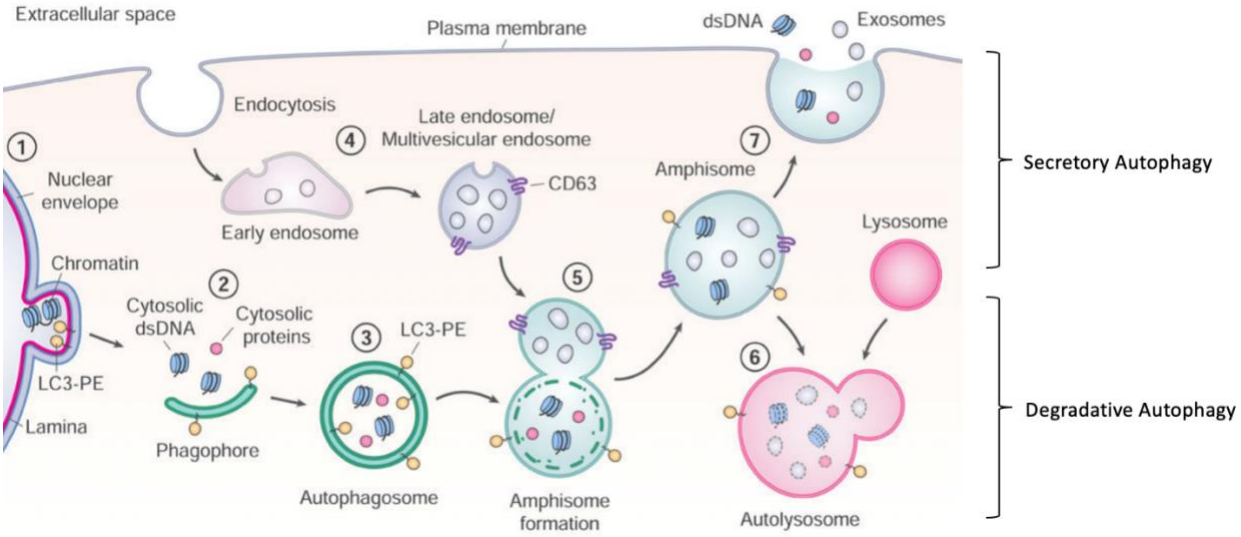

Figure 10. Amphisome Formation Through Autophagy Aathway. Nuclear membranes can bleb, resulting in the formation of cytoplasmic chromatin fragments, due to a mechanism involving LC3B and the nuclear lamina protein Lamin B1. 2) As a phagophore engulfs material, cytoplasmic components are sequestered during autophagy. 3) LC3-PE is required for further autophagic membrane growth, which results in the creation of the double-membrane autophagosome. 4) As early endosomes mature into late endosomes, the pH drops, and the limiting membranes continue to invaginate, resulting in intraluminal vesicles (ILVs). Several ILVs can be found in a fully grown CD63-positive multivesicular endosome (MVE). 5) When an autophagosome fuses with an MVE, the inner autophagosome membrane degrades, resulting in an amphisome, a single-membrane hybrid organelle. 6) The amphisome merges with a lysosomal organelle to produce the autolysosome, which is followed by cargo destruction, or 7) The amphisome fuses with the plasma membrane, triggering extracellular release of dsDNA and histones, as well as the ILVs as exosomes.

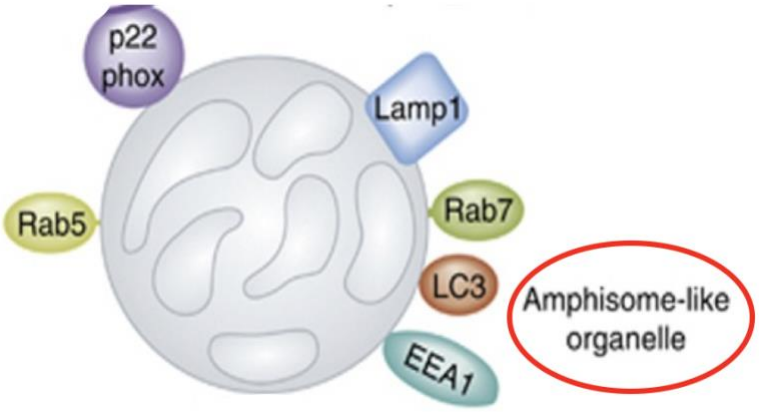

Figure 11. Amphisome-like Organelle. Amphisome is single membrane hybrid organelle which produced through autophagy pathway by fusion of LEs/MVBs with autophagosome. The proteins which are expressing on the surface of amphisome are including:LC3, Lamp1, Rab7, Rab5, EEA1 and p22phox

Kim et al. in their recent study found that before releasing virions, virally infected cells release EVs that include viral proteins and RNA transcripts. Since most lymphocytes, including those infected with HIV-1, are latent in the G0 phase, it is critical to determine whether EVs containing viral proteins and RNA transcripts "prime" recipient cells for the next viral infection cycle and enhance viral spread. Our lab recent work demonstrated that EVs from HIV-1 infected cells released prior to virions, contain viral proteins and RNAs that can activate the cell cycle, making naive recipient T cells and monocytes more susceptible to viral infection in the future [5]. Since the majority of cells, at a cell culture are an unequal mixture of cells at G1, S or G2/M and more than 50% are at G1, to better control of EVs release in this study, we decided to synchronized all the cells at G0 phase by adding serum-deprived media containing 1% serum. After 72

hours the samples were collected, spun and supernatant was saved as 72 hours prior to release or -72 hours samples. Afterward, the cells were released in complete media containing 20% serum, which following that, +6 hours and +24 hours supernatant were collected. Three fractions of HIV-1 infected T-cells and myeloid cells were collected at three different timepoint to be used for further experiments. In the first experiment, we isolated the large EVs of HIV-1 infected T-cells (J1.1) released at +24 hours (**Fig. 1**); next, 2K EVs were purified through Izon column size exclusion chromatography and the fractionated 2K were used for western blot analysis to probe for viral protein p24 and the proteins which are expressing on the amphisome surface, as mentioned above (**Fig. 2**). Data from western blot in **Fig. 3A** revealed that p24 viral protein is strongly expressed in the first fraction (1-5) of 2K EVs which are the largest fractions purified through 35 nm Izon column. In 70 nm column on the other hand, we have the expression of p24, as well as Rab5 protein in the largest fraction (**Fig. 3B**). These data suggest that viral protein and Rab5 are accumulated in the largest fraction of 2K EVs. Moreover, in RT-qPCR data, all three fractions of viral RNA, including TAR, TAR-*gag* and *env* are accumulated in the largest fraction (1-5) of both 35 nm and 70 nm column (**Fig. 4A-B**).

Recent study demonstrated that HIV-1 infected T-cells start to release viral proteins at +6 hours which will be increase overtime up to 24 hours after release (+24 hours) (**Fig. 5**) [5]. In addition, the level of viral RNA also enhanced overtime as far as reached to the highest level at +24 hours (**Fig. 6**). Based on this data, to investigate the infectivity of large EVs released by HIV-1 infected T-cells and myeloid cells, we decided to use +6 hours and +24 hours, as well as 72 hours prior to release samples (-72 hours)

which were not be investigated in our pervious study. RT-qPCR data from **Fig. 7A** demonstrated the presence of all three viral protein in J1.1 2K EVs which released at -72, +6, and +24 hours overtime; which the level of RNA in -72 and +24 hours was higher than +6 hours samples. TAR, TAR-*gag* and *env* are also present in all three fractions of U1 2K EVs; which the level of RNA significantly increased overtime (**Fig. 7B**). Next, we asked whether these three fractions which contain viral RNA are infectious by conducting virus rescue assay. The results from J1.1 2K EVs, in **Fig. 8A** show that previously uninfected cells treated by large EV samples from -72- and +24-hours fractions produced viral proteins gp120, Nef, and p24; but the ones treated with -6 hours fraction did not. In U1 2K samples, (**Fig. 8B**) data also demonstrated the presence of viral protein in -72- and +24-hours fractions. As a result, the +6 hours fraction was found not to be infectious.

Our next experiment involved infectivity assay of large 2K EVs which expressed Lamp1 on the surface. As we mentioned previously, lamp1 is expressing on the surface of amphisome and in this experiment we used immunoprecipitation of Lamp1 antibody to capture the amphisome-like structure. Then, 2K amphisomes at 72 hours prior to release were characterized through an infectivity assay. Western blot results indicated the expression of p24 in the previously uninfected T-cells and myeloid treated by Lamp1-positive 2K EVs secreted from J1.1 (**Fig. 9A**). p24 was also expressed in both CEM and U937 treated by Lamp1-positive 2K EVs released by U1 (**Fig. 9B**). Densitometry count confirmed the p24 expression in the recipient cells which received lamp1-positive 2K particles (**Fig. 9C-D**).

In conclusion, this study revealed that large extracellular vesicles (2K) released from HIV-1 infected myeloid and T-cells, collected at 24 hours post release and from serum-deprived cells (-72 hours), are infectious and contain fully fledged virions, so it can infect nearby uninfected cells. However, Large EVs collected at 6 hours post-release do not contain viral protein, so it failed to initiate viral infection. Moreover, Short non-coding HIV-1 RNA (TAR) is found in 2K fractions, including non-infectious ones (+6 hours), and may play a role in the bystander effect on uninfected neighboring cells. This investigation also suggests that amphisomes, the large vesicles produced during viral infection through autophagy pathway contain fully fledged virions which can infect uninfected neighboring cells.

REFERENCES

[1] G. Sampey, "Exosomes from HIV-1-infected Cells Stimulate Production of Pro-inflammatory Cytokines through Trans-activating Response (TAR) RNA," *J Biol Chem.* , pp. 291(3):1251-1266, 2016.

[2] R. Barclay, "Exosomes from uninfected cells activate transcription of latent HIV-1," *J Biol Chem,* p. 292(28):11682–11701, 2017.

[3] C. DeMarino, "Antiretroviral Drugs Alter the Content of Extracellular Vesicles from HIV-1-Infected Cells," *Sci Rep.,* p. 8(1):7653, 2018..

[4] M. Pleet, "Ebola Virus VP40 Modulates Cell Cycle and Biogenesis of Extracellular Vesicles," *J Infect Dis.,* pp. 218:S365-S387, 2018.

[5] Y. Kim, "Extracellular Vesicles from Infected Cells Are Released Prior to Virion Release," *Cells.* , p. v1;10(4):781, 2021.

[6] J. Kowal, "Proteomic comparison defines novel markers to characterize heterogeneous populations of extracellular vesicle subtypes," *Proc Natl Acad Sci U S A.* , pp. 113(8):E968-E977, 2016.

[7] C. Robert, "the discovery of HIV as the cause of AIDS," *perspectiv,* pp. 2283-2285, 2003. .

[8] "The Global HIV/AIDS Epidemic," *Global Statistics, pp. https://www.hiv.gov/hiv-basics/overview/data-and-trends/global-statistics.*.

[9] N. Archin, "Eradicating HIV-1 infection: seeking to clear a persistent pathogen," *Nat. Rev. Microbiol.,* pp. 12(11): 750-64, 2014.

[10] J. Conway, "Predictions of time to HIV viral rebound following ART suspension that incorporate personal biomarkers," *PLoS Comput Biol,* p. 15(7): e1007229, 2019.

[11] P. Frange, "HIV-1 virological remission lasting more than 12 years after interruption of early antiretroviral therapy in a perinatally infected teenager enrolled in the French ANRS EPF-CO10 paediatric cohort: a case report," *Lancet HIV,* pp. 3(1): e49-54, 2016.

[12] A. Kumar, "Human immunodeficiency virus type 1 RNA Levels in different regions of human brain: quantification using real-time reverse transcriptase-polymerase chain reaction," *J Neurovirol,* pp. 13(3): 210-24, 2007.

[13] H. Hatano, "Cell-based measures of viral persistence are associated with immune activation and programmed cell death protein 1 (PD-1)-expressing CD4+ T cells," *J Infect Dis,* pp. 208(1): 50-60, 2013.

[14] T. Kieffer, "Genotypic analysis of HIV-1 drug resistance at the limit of detection: virus production without evolution in treated adults with undetectable HIV loads," *Infect Dis.,* pp. 1452-65, 2004.

[15] T. Evering, "Absence of HIV-1 evolution in the gut-associated lymphoid tissue from patients on combination antiviral therapyinitiated during primary infection," *PLoS Pathog,* 2012.

[16] E. J. Bunggulawa, "Recent advancements in the use of exosomes as drug delivery systems.," *J Nanobiotechnology,* 2018.

[17] F. Deng, "A review on protein markers of exosome from different bio-resources and the antibodies used for characterization," *J Histotechnol,* pp. 1-14, 2019.

[18] T. Whiteside, "Profiling of plasma-derived extracellular vesicles cargo for diagnosis of pancreatic malignancy," *Ann Tranasl Med,* 2017.

[19] Z. Andreu, "Tetraspanins in Extracellular Vesicle Formation and Function," *Front Immunol 5,* 2014.

[20] D. Murphy, "Extracellular vesicle-based therapeutics: natural versus engineered targeting and trafficking," *Exp Mol Med ,* p. 2019, 51.

[21] W. Fitzgerald, "A System of Cytokines Encapsulated in ExtraCellular Vesicles," *Sci Rep ,* pp. 8: 1-11, 2018.

[22] S.-S. Lee, "A novel population of extracellular vesicles smaller than exosomes promotes cell proliferation," *Cell Commun Signal ,* p. 17, 2019.

[23] K. Gao, "Exosomes Derived From Septic Mouse Serum Modulate Immune Responses via Exosome-Associated Cytokines,"," *Front Immunol,* p. 10, 2019.

[24] C. DeMarino, "Antiretroviral Drugs Alter the Content of Extracellular Vesicles from HIV-1-Infected Cells," *Sci Rep,* pp. 8: 1-20, 2018.

[25] F. Puhm, "Mitochondria Are a Subset of Extracellular Vesicles Released by Activated Monocytes and Induce Type I IFN and TNF Responses in Endothelial Cells," *Circulation Research,* pp. 125: 43-52, 2019.

[26] L. Balaj, " Tumour microvesicles contain retrotransposon elements and amplified oncogene sequences," *Nat Commun ,* p. 2, 2011.

[27] C. Kahlert, "Identification of Double-stranded Genomic DNA Spanning All Chromosomes with Mutated KRAS and p53 DNA in the Serum Exosomes of Patients with Pancreatic Cancer," *J. biol. Chem,* pp. 3869-3875, 2014.

[28] G. D. Johnson, "Chromatin and extracellular vesicle associated sperm RNAs," *Nucleic Acid Res,* pp. 43: 6847-6859, 2015.

[29] G. Storci, "Changes in the biochemical taste of cytoplasmic and cell-free DNA are major fuels for inflamm-aging," *Seminars in Immunology ,* pp. 40: 6-16, 2018.

[30] M. Pleet, "Autophagy, EVs, and Infections: A Perfect Question for a Perfect Time," *Front. Cell. Infect. Microbiol ,* p. 8, 2018.

[31] H. Kalra, "Focus on Extracellular Vesicles: Introducing the Next Small Big Thing," *Int. J Mol. Sci.,* p. 17, 2016.

[32] M. Morello, "Large oncosomes mediate intercellular transfer of functional microRNA," *Cell Cycle* , pp. 12: 3526-3536, 2013.

[33] V. Minciacchi, "Extracellular Vesicles in Cancer: Exosomes, Microvesicles and the Emerging Role of Large Oncosomes," *Semin Cell Dev Biol* , pp. 4: 41-51, 2015.

[34] P. K. Wright, "17beta-estradiol regulates giant vesicle formation via estrogen receptor-alpha in human breast cancer cells," *Oncotarget,* pp. 3055-3065, 2014.

[35] C. Ciardiello, "Large oncosomes overexpressing integrin alpha-V promote prostate cancer adhesion and invasion via AKT activation," *J. Exp. Clin. Cancer Res.,* p. 317, 2019.

[36] A. Yekula, "Large and small extracellular vesicles released by glioma cells in vitro and in vivo," *J. Extracell. Vesicle,* p. 1689784, 2020.

[37] K. Fraser, "Characterization of single microvesicles in plasma from glioblastoma patients," *Neuro Oncol,* pp. 606-615, 2019.

[38] M. Kang, "Roles of CD133 in microvesicle formation and oncoprotein trafficking in colon cancer," *FASEB J.,* pp. 4248-4260, 2019.

[39] M. C. Patton, "Hypoxia alters the release and size distribution of extracellular vesicles in pancreatic cancer cells to support their adaptive survival," *J. Cell. Biochem,* 2019.

[40] M. Surman, "Human melanoma-derived ectosomes are enriched with specific glycan epitopes," *Life Sci,* 2018.

[41] V. R. Minciacchi, *(https://doi.org/10.1080/20013078.2018.1461450),* 2018.

[42] C. Ciardiello, "Focus on extracellular vesicles: new frontiers of cell-to-cell communication in cancer," *Int. J. Mol. Sci.,* p. 17 (2) 175, 2016.

[43] D. DiVizio, "Oncosome formation in prostate cancer: association with a region of frequent chromosomal deletion in metastatic disease," *Cancer Res.,* pp. 5601-5609, 2009.

[44] C. Ciardiello, "Large extracellular vesicles: Size matters in tumor progression," *Cytokine & Growth Factor Reviews,* pp. 51: 69-74, 2020.

[45] H. Pollet, "Plasma membrane lipid domains as platforms for vesicle biogenesis and shedding?," *Biomolecules,* 2018.

[46] B. Brassart, "Tumour cell blebbing and extracellular vesicle shedding: key role of matrikines and ribosomal protein SA," *Br. J. Cancer,* pp. 453-465, 2019.

[47] D. Taylor, "MicroRNA signatures of tumor-derived exosomes as diagnostic biomarkers of ovarian cancer," *Gyneco Oncol.,* pp. 13-21, 2008.

[48] E. D'Asti, "Oncogenic extracellular vesicles in brain tumor progression," *Frontiers in physiology,* 2012.

[49] G. Pezziocoli, "Large Extracellular Vesicles—A New Frontier of Liquid Biopsy in Oncology," *Int. J. Mol. Sci,* 2020.

[50] K. Al-Nedawi, "Intercellular transfer of the oncogenic receptor EGFRvIII by microvesicles derived from tumour cells," *Nat. Cell Biol,* pp. 619-624, 2008.

[51] I. Bertolini, "A GBM-like V-ATPase signature directs cell-cell tumor signaling and reprogramming via large oncosomes," *EBioMedicine,* pp. 41: 225-235, 2019.

[52] A. Nanou, "Leukocyte-Derived Extracellular Vesicles in Blood with and without EpCAM Enrichment," *Cells,* 2019.

[53] A. Hoshino, "Tumour exosome integrins determine organotropic metastasis," *Nature,* pp. 527 (7578), 329-335, 2015.

[54] M. Poggio, "Suppression of exosomal PD-L1 induces systemic anti-tumor immunity and memory," *Cell,* pp. 177 (2), 414-427, 2019.

[55] V. Minciacchi, "MYC mediates large oncosome-induced fibroblast reprogramming in prostate Cancer," *Cancer Res.*, pp. 77 (9), 2306-2317, 2017.

[56] S. Johnson, "Large Extracellular Vesicles Can be Characterised by Multiplex Labelling Using Imaging Flow Cytometry," *Int J Mol Sci,* p. 21(22): 8723, 2020.

[57] U. Demokow, "Extracellular Vesicles in Allergic Rhinitis and Asthma and Laboratory Possibilities for Their Assessment," *Int. J. Mol. Sci.,* pp. 22(5), 2273, 2021.

[58] M. Pleet, "Autophagy, EVs, and Infections: A Perfect Question for a Perfect Time.," *Front. Cell. Infect. Microbiol.,* p. 8, 2018.

[59] H. Klara, "Focus on Extracellular Vesicles: Introducing the Next Small Big Thing," *Int J Mol Sci 17,* 2016.

[60] N. Mizushima, "A brief history of autophagy from cell biology to physiology and disease," *Nature Cell Biology 20,* p. 521–527, 2018.

[61] W. Chang, "Russell, R.C., Tian, Y., Yuan, H., Park, H.ULK1 induces autophagy by phosphorylating Beclin-1 and activating Vps34 lipid kinase," *Nat Cell Biol 15,* p. 741–750, 2013.

[62] R. Kang, "The Beclin 1 network regulates autophagy and apoptosis," *Cell Death Differ ,* pp. 18, 571–580, 2011.

[63] D. Ganesan, "Understanding amphisomes," *biochemical journal,* 2021.

[64] T. Berg, "Isolation and Characterization of Rat Liver Amphisomes," *J. Biol. Chem.,* p. 21883–21892, 1998.

[65] D. Jeppesen, "Reassessment of Exosome Composition," *Cell,* pp. 4;177(2):428-445.e18, 2019.

[66] A. Narayanan, "Exosomes derived from HIV-1-infected cells contain trans-activation response element RNA.," *J Biol Chem,* pp. 288(27):20014-33, 2013.

[67] G. Sampey, "Exosomes and their role in CNS viral infections," *J Neurovirol,* pp. 20(3):199-208, 2014.

[68] D. Klionsky, "Autophagosomes, phagosomes, autolysosomes, phagolysosomes, autophagolysosomes... wait, I'm confused," *Autophagy,* pp. 549-51, 2014.

[69] "Exosomes from HIV-1-infected Cells Stimulate Production of Pro-inflammatory Cytokines through Trans-activating Response (TAR) RNA".

[70] X. Ma, "Essential role for TrpC5-containing extracellular vesicles in breast cancer with chemotherapeutic resistance," *Proc. Natl. Acad. Sci. USA,* pp. 111, 6389-6394, 2014.

[71] A. Nanou, "Circulating tumor cells, tumor-derived extracellular vesicles and plasma cytokeratins in castration-resistant prostate cancer patients," *Oncotarget,* pp. 19283-19293, 2019.

[72] S. Gracia-Silva, "Use of Extracellular Vesicles From Lymphatic Drainage as Surrogate Markers of Melanoma Progression and BRAF V600E Mutation," *J. Exp. Med.,* pp. 216, 1061-1070, 2019.

[73] M. Tucci, "Dual-procedural separation of CTCs in cutaneous melanoma provides useful information for both molecular diagnosis and prognosis," *Ther. Adv. Med. Oncol.,* 2020.

[74] H. Julish-Haertel, "Cancer-associated circulating large extracellular vesicles in cholangiocarcinoma and hepatocellular carcinoma," *J. Hepatol,* pp. 67, 282-292, 2017.

[75] Z. Kassam, "A prospective feasibility study evaluating the role of multimodality imaging and liquid biopsy for response assessment in locally advanced rectal carcinoma," *Abdom. Radiol.,* pp. 44, 3641-3651, 2019.

[76] T. Lattanze, "Detection and assessment of nuclear material associated with extracellular vesicles from HTLV-1 infected cells," 2019.

[77] N. Shafagati, "The use of Nanotrap particles for biodefense and emerging infectious disease diagnostics," *Pathog Dis,* pp. 71(2):164-76, 2014.

[78] M. Thali, "The roles of tetraspanins in HIV-1 replication.," *Curr Top Microbiol Immunol,* pp. 339:85-102, 2009.

[79] H. Suarez, "Tetraspanins, Another Piece in the HIV-1 Replication Puzzle.," *Front Immunol,* p. 9:1811, 2018.

BIOGRAPHY

Fatemeh Dehbandi graduated from Azad University of Babol with her BS in biology (with a concentration in cellular and molecular biology) in 2016. She then went on to work at Gastrointestinal and liver diseases research center (GLDRC) in Guilan University of Medical Sciences from 2016 to 2018 as a researcher.